

2008

Comparing the volume swell of fluorosilicone o-rings with the quantitative analysis of absorbed jet fuel

George William Fels
University of Dayton

Follow this and additional works at: https://ecommons.udayton.edu/graduate_theses

Recommended Citation

Fels, George William, "Comparing the volume swell of fluorosilicone o-rings with the quantitative analysis of absorbed jet fuel" (2008). *Graduate Theses and Dissertations*. 2622.
https://ecommons.udayton.edu/graduate_theses/2622

This Thesis is brought to you for free and open access by the Theses and Dissertations at eCommons. It has been accepted for inclusion in Graduate Theses and Dissertations by an authorized administrator of eCommons. For more information, please contact mschlangen1@udayton.edu, ecommons@udayton.edu.

COMPARING THE VOLUME SWELL OF FLUOROSILICONE O-RINGS WITH
THE QUANTITATIVE ANALYSIS OF ABSORBED JET FUEL

Thesis

Submitted to

The School Of Engineering

UNIVERSITY OF DAYTON

In Partial Fulfillment of the Requirements for

The Degree

Master of Science in Chemical Engineering

by

George William Fels

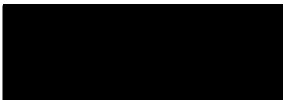
UNIVERSITY OF DAYTON

Dayton, Ohio


May, 2008

COMPARING THE VOLUME SWELL OF FLUOROSILICONE O-RINGS WITH
THE QUANTITATIVE ANALYSIS OF ABSORBED JET FUEL


APPROVED BY:




Kevin J. Myers, D.Sc., P.E.
Professor
Chemical and Materials
Engineering Department
Committee Chairman



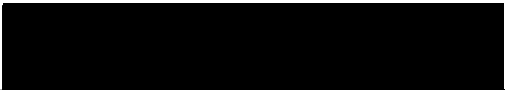
John L. Graham, Ph.D.
University of Dayton
Research Institute
Research Advisor



Charles E. Browning, Ph.D.
Professor and Torley Chair
Chemical and Materials
Engineering Department
Committee Member



Donald K. Minus
Air Force Research Laboratory
Committee Member



Malcolm W. Daniels, Ph.D.
Associate Dean
School of Engineering



Joseph E. Saliba, Ph.D., P.E.
Dean
School of Engineering

ABSTRACT

COMPARING THE VOLUME SWELL OF FLUOROSILICONE O-RINGS WITH THE QUANTITATIVE ANALYSIS OF ABSORBED JET FUEL

George William Fels
University of Dayton, 2008

Research Advisor: Dr. John L. Graham
Academic Advisor: Dr. Kevin J. Myers

In this study, quantitative analysis was performed to determine the change in volume of a polymeric material in the presence of surrogate jet propulsion (JP) and Fischer-Tropsch (FT) fuels. Changes in volume of fluorosilicone polymer O-rings, aged in various test fluids, obtained from standardized methods were directly compared to its change in mass as determined by the quantitative analysis from a direct thermal desorption Gas Chromatography – Mass Spectrometry (GC-MS) system. A previous material compatibility study conducted on nitrile rubber found a strong linear relationship between the measured fuel volume absorbed by the GC-MS technique and a standardized method. However, the GC-MS analysis indicated more fluid was absorbed than the standardized method had measured. This study was a carefully designed comparison of these two techniques.

To examine the apparent discrepancy, the volume swell was measured by ASTM D – 471 and the volume of absorbed fuel found by the GC-MS method

were compared. The study was conducted using test fluids ranging in complexity from 1 to 8 components, one FT fuel, and one JP fuel. The test material was fluorosilicone because it contained no extractable plasticizer and showed significant volume swell. The results of this study showed the GC-MS method indicated more fuel being absorbed by the polymer than indicated by the measured volume swell by 20% as compared to the 60% that was found from a previous study. The GC-MS technique was found to provide a more accurate measurement of the contributions of individual fuel components to the volume swell of the polymer. It was also determined that measurements from the previous study were made under non-equilibrium conditions. The molecular interactions between the fluid and polymer had not ceased before the measurements were made, accounting for much of the discrepancy. Proper calibration of the system's response to each test fluid also was determined to be a critical part from this study.

Further investigation of various test fluids and materials should be conducted to refine the methods and procedures described in this study.

ACKNOWLEDGEMENTS

I would like to gratefully acknowledge the support of the U.S. Air Force Research Laboratory, Propulsion Directorate, Propulsion Sciences and Advanced Concepts Division, Wright-Patterson Air Force Base, Ohio, and under Contract No. F33615-03-2-2347 (Technical Monitor: Mr. Bob Morris) for funding this study. (The views and conclusions contained herein are those of the authors and should not be interpreted as necessarily representing the official policies or endorsements, either expressed or implied, of the Air Force Research Laboratory or the U.S. Government.)

I would like to thank Dr. John Graham for his consistent guidance in this area of study. I attribute my success in this work to his patience, encouragement, and confidence in my ability. A special thanks goes to my co-advisor, Dr. Kevin Myers, for his endless support through this work and my previous academic years. I would like to thank the rest of my thesis committee: Dr. Charles Browning and Mr. Donald Minus for their time and insightful comments. I am indebted to the University of Dayton Research Institute's Environmental Engineering Group for their constant willingness to help and provide encouragement. Lastly, I would like to extend my gratitude to my family and friends for their love and consistent support.

TABLE OF CONTENTS

| | |
|--|-----|
| ABSTRACT..... | iii |
| ACKNOWLEDGEMENT..... | v |
| LIST OF FIGURES..... | vii |
| LIST OF TABLES..... | x |
| <u>CHAPTER</u> | |
| I. INTRODUCTION..... | 1 |
| II. BACKGROUND..... | 6 |
| III. EXPERIMENTAL APPROACH..... | 13 |
| Materials..... | 13 |
| Experimental Methods | |
| Volume Swell..... | 16 |
| Direct Thermal Desorption GC-MS..... | 19 |
| IV. RESULTS AND DISCUSSION..... | 23 |
| Two Sample t -Test..... | 24 |
| Paired Difference..... | 29 |
| V. CONCLUSIONS AND ECOMMENDATIONS..... | 32 |
| APPENDIX..... | 34 |
| REFERENCES..... | 63 |

LIST OF FIGURES

| <u>Figure</u> | <u>Page</u> |
|---|-------------|
| 1 A typical JP-8 (a) and an FT fuel (b) chromatogram..... | 7 |
| 2 Summary of the volume of absorbed fuel analyzed by GC-MS versus the measured volume swell of nitrile rubber O-rings (Parker N0602-70-001) aged in fuel..... | 11 |
| 3 Volume swell as a function of time for nitrile rubber exposed to selected JP and FT fuels..... | 11 |
| 4 Chromatographic progression of the five test fluids..... | 15 |
| 5 Method of weighing the O-ring sample in air (a) and submerged in distilled water (b)..... | 17 |
| 6 The immersion apparatus used to age the fluorosilicone O- rings in a test fluid..... | 18 |
| 7 The System for Thermal Diagnostic Studies (STDS)..... | 19 |
| 8 Inside view of the desorption oven..... | 20 |
| 9 Volume of fuel absorbed by a single O-ring immersed in each fuel by method D-471..... | 23 |
| 10 Volume contributions of the absorbed fluid for the individual components of Fluids A, B, and C..... | 26 |
| 11 Average volume swell of each test fluid and the 90% confidence intervals..... | 28 |
| 12 Average paired difference of each test fluid and the 90% confidence intervals..... | 31 |

| | | |
|------|---|----|
| 13 | Fuel absorbed versus volume swell for nitrile rubber O-rings aged for 40 hours at room temperature. Prior to aging in fuel the plasticizer had been removed from these O-rings..... | 33 |
| A.1 | Calibration curve (above) and calculations (below) for O-ring 1 in Fluid A..... | 35 |
| A.2 | Calibration curve (above) and calculations (below) for O-ring 2 in Fluid A..... | 36 |
| A.3 | Calibration curve (above) and calculations (below) for O-ring 3 in Fluid A..... | 37 |
| A.4 | Calibration curve (above) and calculations (below) for O-ring 4 in Fluid A..... | 38 |
| A.5 | Calibration curves for Toluene (above) and Dodecane (below) for O-ring 1 in Fluid B..... | 39 |
| A.6 | Calibration curves for Toluene (above) and Dodecane (below) for O-ring 2 in Fluid B..... | 41 |
| A.7 | Calibration curves for Toluene (above) and Dodecane (below) for O-ring 3 in Fluid B..... | 43 |
| A.8 | Calibration curves for Toluene (above) and Dodecane (below) for O-ring 4 in Fluid B..... | 45 |
| A.9 | Fluid C component calibration curves for O-ring 1..... | 47 |
| A.10 | Fluid C component calibration curves for O-ring 2..... | 49 |
| A.11 | Fluid C component calibration curves for O-ring 3..... | 51 |
| A.12 | Fluid C component calibration curves for O-ring 4..... | 53 |
| A.13 | Calibration curve (above) and calculations (below) for O-ring 1 in FT fuel..... | 55 |
| A.14 | Calibration curve (above) and calculations (below) for O-ring 2 in FT fuel..... | 56 |
| A.15 | Calibration curve (above) and calculations (below) for O-ring 3 in FT fuel..... | 57 |

| | | |
|------|--|----|
| A.16 | Calibration curve (above) and calculations (below) for O-ring 4 in FT fuel..... | 58 |
| A.17 | Calibration curve (above) and calculations (below) for O-ring 1 in JP-8 fuel..... | 59 |
| A.18 | Calibration curve (above) and calculations (below) for O-ring 2 in FT fuel..... | 60 |
| A.19 | Calibration curve (above) and calculations (below) for O-ring 3 in FT fuel..... | 61 |
| A.20 | Calibration curve (above) and calculations (below) for O-ring 4 in FT fuel..... | 62 |

LIST OF TABLES

| <u>Table</u> | | <u>Page</u> |
|--------------|---|-------------|
| 1 | Top World Oil Producing/Consuming Countries, 2006 (thousand barrels per day)..... | 1 |
| 2 | Top World Oil Net Importers/Exporters, 2006 (thousand barrels per day)..... | 3 |
| 3 | Composition of selected test fluids | 14 |
| 4 | Fluid component contributions to the volume of fuel absorbed measured by the GC-MS method..... | 25 |
| 5 | Individual volume swell of each O-ring by ASTM D – 471 and by direct thermal desorption using a GC-MS..... | 27 |
| 6 | Volume swell results from the two sample <i>t</i> -test on each test fluid..... | 28 |
| 7 | Results of paired difference displaying confidence intervals..... | 30 |
| A.1 | ASTM D – 471 source data measurements..... | 34 |
| A.2 | Calculations for O-ring 1 in Fluid B..... | 40 |
| A.3 | Calculations for O-ring 2 in Fluid B..... | 42 |
| A.4 | Calculations for O-ring 3 in Fluid B..... | 44 |
| A.5 | Calculations for O-ring 4 in Fluid B..... | 46 |
| A.6 | Calculations for O-ring 1 for Fluid C..... | 48 |
| A.7 | Calculations for O-ring 2 for Fluid C..... | 50 |
| A.8 | Calculations for O-ring 3 for Fluid C..... | 52 |

| | | |
|-----|--|----|
| A.9 | Calculations for O-ring 4 for Fluid C..... | 54 |
|-----|--|----|

CHAPTER I

INTRODUCTION

A critical component of the global economy is the availability of crude oil. According to the Energy Information Administration (EIA), 84.7 million barrels per day (mmbd) were consumed globally in 2006.¹ The United States is consuming nearly one-quarter of the petroleum produced (Table 1) and with a rapidly expanding global economy, it is estimated that the world oil demand will expand by 40% in the next 15 – 20 years.²

Table 1. Top World Oil Producing/Consuming Countries, 2006.³
(thousand barrels per day)

| Rank | Production | | Consumption | |
|------|---------------|--------|---------------|--------|
| 1 | Saudi Arabia | 10,665 | United States | 20,687 |
| 2 | Russia | 9,677 | China | 7,273 |
| 3 | United States | 8,331 | Japan | 5,159 |
| 4 | Iran | 4,148 | Russia | 2,920 |
| 5 | China | 3,845 | Germany | 2,665 |
| | World Total | 84,600 | World Total | 84,770 |

It is projected that the world's consumption of petroleum will increase from 85 million barrels in 2006 to 118 million barrels in 2030 as the world maintains rapid economic growth.² These projections may show a greater demand of petroleum than the world's top oil producing countries can provide, spurring a worldwide debate on the concept of 'peak oil.

The American geologist M. King Hubbert predicted a plateau in U.S. oil production or 'peak oil'. In 1956, Hubbert's prediction stated the U.S. oil production will peak in the early 1970s and decline thereafter.⁴ As the U.S. experienced the greatest production in 1970, his analysis has since been proved to be accurate. In 1969, Hubbert then predicted that annual world oil production would peak in the year 2000.⁵ But according to Kenneth Deffeyes, the world oil production peaked in 2005. But other analysts believe it will not do so for the next 10-15 years.⁶ Regardless, the world's oil supply is a finite resource that may not match the world's future demand. The concept of peaking world oil production creates fears of price escalations, fuel shortages, and the onslaught of a global economic and political crisis.⁷

At the end of 2005, the Organization of Petroleum Exporting Countries (OPEC) controlled 75% of all proven oil reserves in the world.⁸ As of September 2007, nearly 45% of all U.S. petroleum was imported from OPEC nations such as Nigeria, Saudi Arabia, Venezuela, and Iraq.⁹ Table 2 presents the top countries importing and exporting petroleum. To reduce America's dependence on oil from foreign nations and to prepare for a possible decline in world oil production requires implementing recent technological developments in fuel efficiency and renewable sources.

One possible way to reduce dependence on foreign oil could be America's vast resources of coal. The U.S. contains more than one-quarter of the world's identified coal reserves.¹⁰ In the President's 2007 Budget, more than \$280

Table 2. Top World Oil Net Importers/Exporters, 2006.³
(thousand barrels per day)

| Rank | Imports | | Exports | |
|------|---------------|--------|------------------------|-------|
| 1 | United States | 12,357 | Saudi Arabia** | 8,525 |
| 2 | Japan | 5,031 | Russia | 6,757 |
| 3 | China | 3,428 | United Arab Emirates** | 2,564 |
| 4 | Germany | 2,514 | Norway | 2,551 |
| 5 | South Korea | 2,156 | Iran** | 2,487 |

**OPEC Member

million was proposed for investments in innovative coal technologies aimed towards reducing the demand of petroleum and to provide cleaner alternative liquid fuels.¹⁰

One such investment is an almost century old technique. A synthesis of a liquid hydrocarbon fuel from coal, or natural gas, has the potential to provide an alternative to conventional petroleum distillate fuels. An extension on coal gasification during World War I led to the synthesis of a new liquid transportation fuel. The work done in the 1920s by Franz Fischer and Hans Tropsch converted synthesis gas from coal gasification into liquid hydrocarbons in the presence of a catalyst. The liquid fuel resembled a petroleum distillate fuel capable of reducing Germany's fuel shortage during the war. Currently, the availability of the country's vast coal reserves has made this process appealing to the U.S. Department of Defense (DOD) as a possible alternative source of jet fuel.¹¹

The DOD consumed 844 trillion Btu (149 million barrels) of energy in 2006, corresponding to only 1% of the 100 quadrillion Btu of energy the United States requires annually.¹² In 2005, the United States Air Force (USAF) spent \$4 billion on 3.2 billion gallons of jet fuel and typically consumes 10% of the jet fuel

produced annually for the U.S. aviation market.¹³ As petroleum prices and security issues escalate, an increasing need for petroleum alternatives has led the USAF to study a more affordable and secure fuel source. Hydrocarbon fuels produced by the Fischer-Tropsch (FT) process can contribute to achieving a jet fuel alternative.

One challenge of integrating alternative sources of liquid transportation fuels into the aviation industry and then into fuel systems is with material compatibility. The compositional differences between FT fuels and JP fuels in operation today are reasons for further investigation. For example, unlike conventional JP fuels, FT fuels are composed of only complex paraffins and isoparaffins. Aromatics, present in JP fuels and not in FT fuels, can be preferentially absorbed into elastomer O-rings throughout the aircraft's fuel system. If FT fuels are incorporated into the fuel system, the lack of aromatics may cause polymers throughout the system to shrink and harden, inevitably leading to an improper seal.¹⁴ It is important to develop an approach to anticipate and understand how fuels interact with various polymeric materials.

A technique used to measure the interactions between jet fuels and polymeric materials is the volume swell of the polymer. Being capable of quantifying specific components absorbed into the polymer will provide an understanding of how the absorbed species affect the swell of the material.

Early test methods were limited to determining the overall fuel contribution by measuring the volume swell. But now a method of direct thermal desorption using a gas chromatograph-mass spectrometer (GC-MS) allows the selected

absorbed fuel components to be identified and quantified. It allows each fuel component to be assigned its contribution to the overall volume swell of the polymeric material. A close examination of previous data has shown a significant discrepancy between the volume swell and thermal desorption methods. In order to evaluate the differences of these two analyses, a series of designed experiments were conducted to quantitatively compare the two methods of measuring the absorbed fuel volume.

CHAPTER II

BACKGROUND

The DOD has great interest in gaining energy independence from foreign fuel sources by indentifying a more secure, affordable, and stable fuel alternative. Coal-to-Liquid technology (CTL), such as that pioneered by the Fischer-Tropsch synthesis, produces a complex low-sulfur, low aromatic hydrocarbon fluid containing linear and branched alkanes. During this synthesis, hydrocarbon feedstocks (typically coal or natural gas) are broken down at elevated temperatures into carbon monoxide (CO) and hydrogen (H₂) called synthesis gas. This gas mixture is then recombined over an appropriate catalyst, usually cobalt or iron, producing straight and branched alkanes.¹⁵

In contrast to FT fuels, conventional aviation and jet propulsion fuels are primarily composed of complex petroleum-derived hydrocarbon chains. The fuel composition is mainly composed of three main classes of hydrocarbons, typically 20% aromatics, 60% alkanes (linear and branched), and 20% cycloalkanes (naphthenes).¹¹ Heteroatomic species, such as sulfur, nitrogen, and/or oxygen, play an important role in thermal stability, lubricity, and storage stability of the fuel and total less than 1% of the jet fuel.¹⁶ As the USAF pushes toward coal-derived hydrocarbons, the compositional differences between synthetic FT and JP fuels present issues of material compatibility within the aircraft's fuel system. The

chromatograms of the two fuels illustrated in Figure 1 display a similar boiling range and fluid complexity but analysis confirms the difference in fuel compositions.

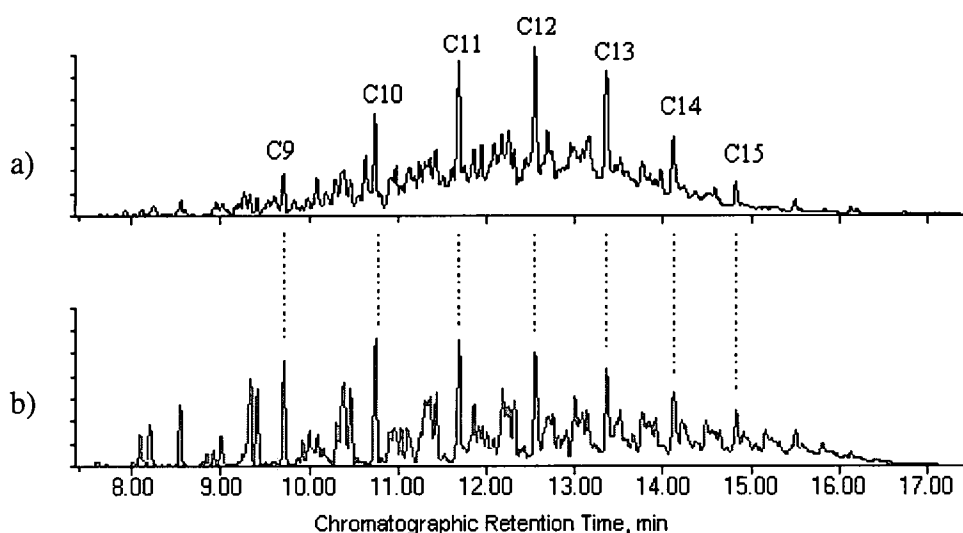


Figure 1. A typical JP-8 (a) and an FT fuel (b) chromatogram.

Typical JP and FT fuels are relatively non-polar fluids and are considered relatively mild solvents with respect to the polymers used throughout the fuel system. Polymers, in the presence of solvents, begin to slowly absorb the solvent in contact, forming a gel-like solution. These gel-like polymer solutions can give insight into the intermolecular interactions such as polymer chain disentanglement and fuel diffusivity.¹⁷ An exchange of material, either fuel absorption or polymer extraction, is a result of the interactions between the fuel and polymer. The interactions are dependent upon the intermolecular

characteristics, like the fuel's polarity and molar volume, between the polymer and the fuel.

The process must first be thermodynamically favorable if components are preferentially absorbed into or are extracted from the polymer. The formation of the polymer solution is governed by the free energy of mixing:¹⁷

$$\Delta G_m = \Delta H_m - T \Delta S_m$$

where ΔG_m is Gibbs' free energy of mixing, ΔH_m is the change in enthalpy, ΔS_m is the change in entropy, and T is the absolute temperature. The crucial factor in determining the interaction between the polymer and the solvent is the sign of the Gibbs free energy change.

In absorption, the Gibbs free energy will be negative forcing components into the polymer and inevitably shifting the balance of equilibrium. Once the thermodynamic conditions are present, the process of forming a polymer solution consists of three sequential steps. First, polymer-polymer intermolecular bonds must break and create a cavity able to accommodate fuel molecules and the fuel-fuel intermolecular bonds must break in order to penetrate the polymer. Finally, polymer-fuel intermolecular bonds are then formed releasing energy once the fuel molecule is inserted into the polymer.¹⁸ Only when equilibrium is reached ($\Delta G_m=0$) will net intermolecular movements cease.

The compatibility between the polymer and the solvent may be predicted by the use of solubility parameters which account for specific intermolecular bonding characteristics. The enthalpy change of mixing corresponds to the energy associated with making and breaking of intermolecular bonds described

by the solubility parameters. The Hildebrand solubility parameter was first used to devise an estimate for the intermolecular interactions between substances, but specific interactions such as hydrogen bonding and the percentage of cross-linkage were not considered.¹⁷ Hansen solubility parameters (HSPs), on the other hand, account for the molecular interactions in terms of dispersive, polar, and hydrogen bonding forces that are present between the fuel and polymer.¹⁹ Because polymers typically used in fuel systems are often relatively polar, it is generally energetically unfavorable to break their intermolecular bonds in exchange for weaker nonpolar JP-fuel bonds. But it is possible for individual components within JP fuel to have similar polar characteristics capable of creating a fuel-polymer interaction. For instance, aromatics have similar polar and hydrogen-bonding solubility parameters as polymers, thus resulting in intermolecular exchanges. This interaction between the polymer and solvent will initiate disentanglement of polymer chains leading to the absorption of solvent components contributing to an increase in polymeric volume (i.e. swell).

Polymer O-rings are common penetrable materials throughout an aircraft's fuel system and are the main material focused on in this study. Direct thermal desorption is a unique test method for indentifying a fuel component's contribution to volume change of the polymer O-rings. The absorbed fuel is thermally desorbed from the aged polymer O-ring and then analyzed by a gas chromatograph-mass spectrometer (GC-MS) determining the identity and the volume contribution for each individual fuel component. The GC-MS technique

relates the volume contributions of fuel components to the volume swell undergone by the polymer.

The actual volume absorbed by the O-ring can be measured by a standard test method. ASTM method D – 471 measures the volume swell of rubber and rubber-like materials when exposed to test liquids.²⁰ The volume swell is calculated by weighing the aged O-ring in air and then submerged in water. This study will correlate the quantitative response of absorbed fuel from the GC-MS analysis with the measured volume swell of D – 471.

Nitrile rubber is one of the most extensively studied materials with respect to material compatibility. A past study, conducted on nitrile rubber aged in various jet fuels, compared the volume swell data with the GC-MS data. The data displayed a strong linear correlation between the GC-MS technique and a standard swell test method. Figure 2 presents the graph of the percentage of absorbed fuel analyzed by GC-MS plotted against the measured volume swell.²¹ The figure displays two discrepancies related to the two methods: an offset (non-zero intercept) and a slope of best fit exceeding unity. The offset was created from the extraction of plasticizer from the nitrile rubber O-rings. This effect can be seen in Figure 3 as the volume swell gradually decreases as the plasticizer is continuously extracted during the 16 hour exposure time. The surprising and significant aspect of Figure 2 is the lack of a 1:1 correlation between the two volume swell techniques. While the data illustrates a strong correlation between the GC-MS technique and the volume swell analysis, the GC-MS data does not reflect the observed volume change of

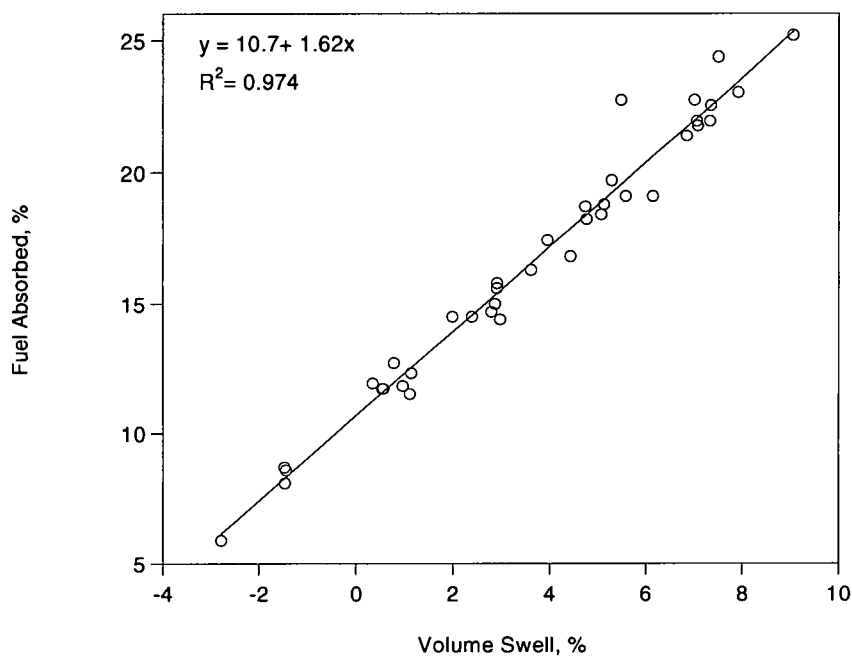


Figure 2. Summary of the volume of absorbed fuel analyzed by GC-MS versus the measured volume swell of nitrile rubber O-rings (Parker N0602-70-001) aged in fuel.²¹

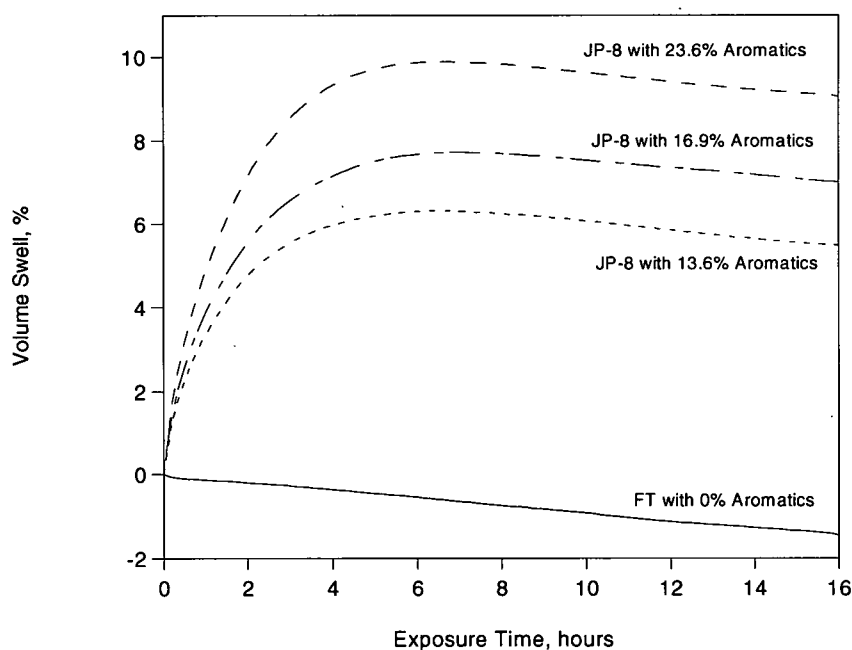


Figure 3. Volume swell as a function of time for nitrile rubber exposed to selected JP and FT fuels.²¹

the material. Specifically, the slope of 1.62 suggests the material absorbed 62% more fuel than the actual volume swell data indicated.²¹

This discrepancy between the GC-MS and the measured volume swell must be reconciled before specific contributions by the GC-MS can be assigned to individual fuel components associated with a volume increase. It is not known whether the differences of the two methods are related to a physical or an experimental issue between the techniques, but possible differences could be attributed to non-ideal solutions or that a state of equilibrium was not reached between the fuel and polymer before the two methods were conducted. Therefore, the purpose of this study is to evaluate and compare the measured volume change of polymer O-rings in several test fluids with the corresponding quantitative analysis of the absorbed fluid to help understand the observed discrepancies illustrated in Figure 2.

CHAPTER III

EXPERIMENTAL APPROACH

Materials

The O-rings used in the study were fluorosilicone L1120-70-214 (Parker Hannifin Corp., Lexington, KY). These O-rings were nominally 2.499 cm in inner diameter and 0.353 cm in cross section. In part, fluorosilicone (polymethyl-3,3,3-trifluoropropyl siloxane) was selected as it contains no plasticizer or other additives which can be extracted from the polymer, simplifying the data analysis. Also, fluorosilicone shows measurable volume swell in both polar and non-polar solvents like FT and JP jet fuels. The source O-rings from the supplier were analyzed by the direct thermal desorption technique to ensure the samples were free of plasticizers, contaminants, and other additives.

Five test fluids were used: three solvent mixtures with 1 to 8 components, one FT and one JP-8 fuel. The test fluids were used as received from the supplier (Sigma-Aldrich Co., St. Louis, MO) and blended as shown in Table 3. The FT fuel was produced by Syntroleum Corporation in Tulsa, Oklahoma (POSF 4909), to have the same physical properties as a typical JP-8 fuel, but with no aromatics. A nominal JP-8 fuel (POSF 4177) provided by the U.S. Air

Force Research Laboratory at Wright Patterson Air Force Base (WPAFB) in Dayton, Ohio, contained 16.9% aromatics.

Table 3. Composition of selected test fluids.

| | | | |
|----------------|------------------------------------|----------------|------------|
| Fluid A | n-Dodecane | $C_{12}H_{26}$ | 100% |
| Fluid B | Toluene | C_7H_8 | 30% |
| | n-Dodecane | $C_{12}H_{26}$ | 70% |
| Fluid C | Aromatics | | 25% |
| | n-Butylbenzene | $C_{10}H_{14}$ | 5% |
| | 1,2,3,4-Tetrahydronaphthalene | $C_{10}H_{12}$ | 10% |
| | 1-Methylnaphthalene | $C_{11}H_{10}$ | 10% |
| | Paraffins | | 53% |
| | n-Decane | $C_{10}H_{22}$ | 15% |
| | n-Dodecane | $C_{12}H_{26}$ | 23% |
| | n-Tetradecane | $C_{14}H_{30}$ | 15% |
| | Cycloparaffins | | 22% |
| | Decahydrohaphthalene (cis + trans) | $C_{10}H_{18}$ | 11% |
| | n-Butylcyclohexane | $C_{10}H_{20}$ | 11% |

Fluid A was a single component fluid modeled after hydrocarbon fluid Type I.²² The Type I reference fluid is typically comprised of 100% isooctane, but relatively high volatility made this fluid difficult to work with, so isooctane was replaced with dodecane. Similarly, Fluid B was a two component test fluid modeled after hydrocarbon fluid Type III consisting of 30% toluene in isooctane.²³ The isooctane was substituted with dodecane to decrease the fluid's volatility. The 8 compounds of Fluid C were selected to represent the major components found in JP-8; linear and cyclic alkanes and single- and double-ring aromatics.²⁴ The exact composition of Fluid C was established from recommendations of

researchers at the U.S. Air Force Research Laboratory's Fuels Branch at WPAFB in Dayton, Ohio.

Figure 4 displays the progression in complexity of the test fluids from a single component Fluid A through to the complex FT and JP-8 fuels.

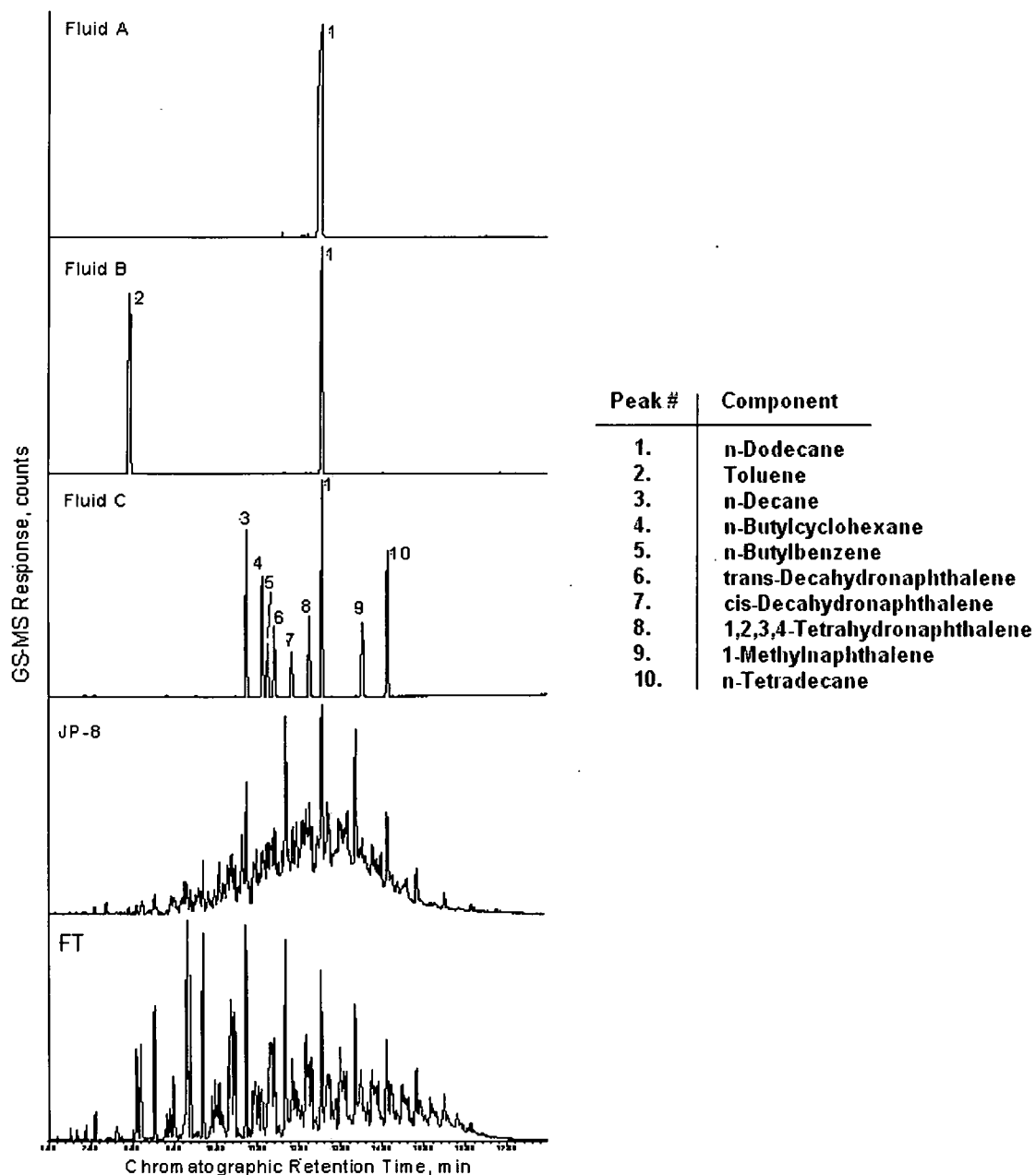


Figure 4. Chromatographic progression of the five test fluids.

Experimental Methods

Volume Swell

Measuring the change in volume of a polymer material can be performed by following the test method ASTM D – 471 – 98.²⁰ This test evaluates the ability of rubber and rubber-like materials to withstand the effect of liquids. Briefly, this method is based on measuring the weight of a sample in air and while immersed in water (Figure 5). The weight difference provides the weight of the water displaced by the sample, and hence its volume is calculated. Measuring the initial and final volume of a fluorosilicone O-ring before and after an elapsed time can provide the volume swell or shrinkage experienced by the sample. Section 11 in ASTM method D – 471 was followed precisely to obtain the change in volume. Specifically, the change in volume can be found as:

$$\Delta V, \% = \frac{(M_3 - M_4) - (M_1 - M_2)}{(M_1 - M_2)} \cdot 100\% \quad (3.1)$$

where M_1 is the initial mass (g) of the specimen in air, M_2 is the initial mass (g) of the specimen immersed in water, M_3 is the mass (g) of the specimen in air after equilibrium is reached, and M_4 is the mass (g) of the specimen in water after the appropriate immersion period.

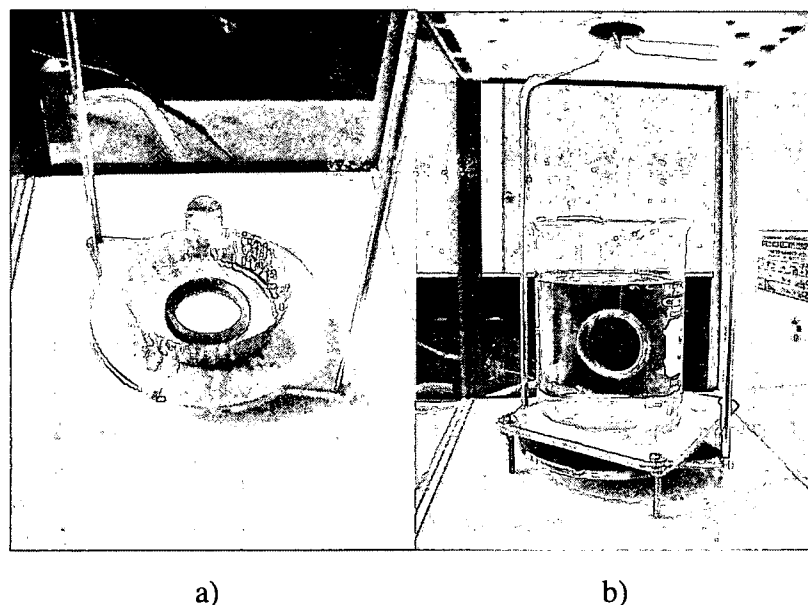


Figure 5. Method of weighing the O-ring sample in air (a) and submerged in distilled water (b).

The volume swell measurement for all five test fluids was performed on four separate O-rings. Each of the four O-rings was initially weighed dry in air on a five-place Mettler model H20 analytical balance (Figure 5a). Next, each O-ring specimen was weighed while immersed in deionized water at room temperature to obtain the sample's water displacement (Figure 5b). Each sample was then quickly dipped in methanol to expel the water, blotted dry with a laboratory tissue, and the samples were placed in an immersion apparatus containing the appropriate bulk fluid. As shown in Figure 6, a simple vessel was assembled to separate and completely suspend the specimens in the fluid using a set of aluminum hooks.



Figure 6. The immersion apparatus used to age the fluorosilicone O-rings in a test fluid.

During the immersion period, one O-ring from each fuel was weighed daily to monitor the absorption of fluid. By blotting the O-ring sample gently and allowing the least possible lapse time in air to ensure little liquid evaporation, the weight of the specimen was measured. The immersion period concluded when the reference O-ring ceased to change weight indicating that polymer-fuel equilibrium was reached. The change in volume of each of the four O-rings was then measured as described above.

Direct Thermal Desorption GC-MS

The fluid absorbed by each fluorosilicone O-ring sample was quantitatively analyzed using a System for Thermal Diagnostic Studies (STDS).²⁵ The STDS consists of two Agilent 5890 temperature programmed gas chromatograph ovens connected in series (Figure 7).

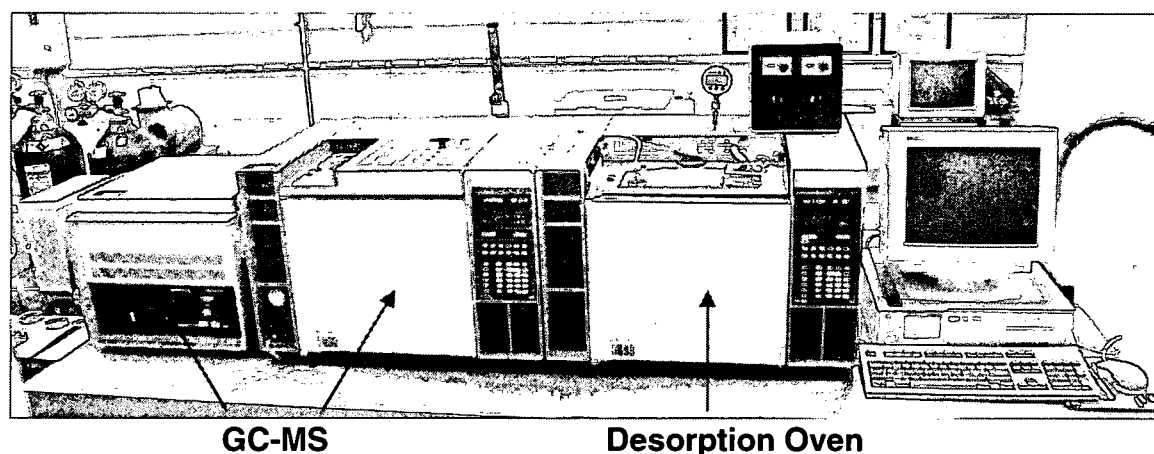


Figure 7. The System for Thermal Diagnostic Studies (STDS).

The desorption oven contained a thermal desorption cell for vaporizing the absorbed fluid from the O-ring samples. The second oven was configured as a conventional gas chromatograph-mass spectrometer (GC-MS) for the identification and quantitation of the absorbed species. The desorption cell (Figure 8) consisted of a 4" length x $\frac{1}{4}$ " diameter nickel tube connected to a $\frac{1}{16}$ " silicosteel (Restek, Bellefonte, PA) transfer line to the GC-MS through a 200:1 split flow inlet.

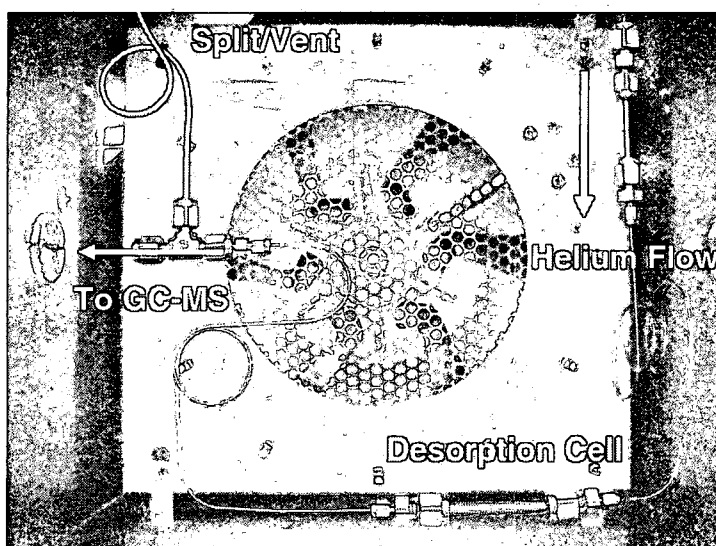


Figure 8. Inside view of the desorption oven.

Dry helium flowing through the desorption cell was regulated by two independent differential flow controllers (Model VDC 1000, Porter Instrument Co.). The GC-MS was fitted with a DB-1 chromatograph capillary column of 0.2 mm x 25 m (J&W Scientific; Folsom, CA) with a film thickness of 0.33 μm . The MS was an Agilent 5970B Mass Selective Detector (MSD) scanning from 35 to 350 AMU with an electron multiplier potential of 1800 VDC.

The same O-rings as measured by D – 471 were used as samples for the analysis of absorbed fluid. Samples were prepared by cutting small sections from each O-ring (500-2000 μg) and sealing them in a 1.8 mL glass vial with 1.0 mL of the corresponding fluid. For each analysis, a sample was removed from the fluid, dabbed dry with a laboratory tissue, and placed in the desorption cell. The desorption oven was then heated from 30°C to 250°C at a rate of 20°C/min and held at 250°C for 10 minutes. Dry helium flowing at 34 mL/min transported the vaporized fluid to the GC-MS which was held at -30°C. Upon the completion

of the transfer of material to the GC-MS, the flow of helium to the system was reduced to 10 mL/min by switching off one of the two differential flow controllers and a pressurization coil affixed to the split vent raised the column head pressure to 3.7 psig (Ashcroft Digital Test Gauge, Model 2089). The GC-MS was then heated from -30°C to 280°C at a rate of 20°C/min and held for 10 minutes. After every sample, the pressurization coil was flushed with solvent to ensure consistent analytical conditions.

The fluid samples were analyzed in a similar manner. Briefly, the fluid samples were diluted with hexane ($\geq 99\%$, Sigma-Aldrich Co.) and injected onto the desorption cell with a 1.0 μL GC syringe (Hamilton 7000 Series). After each analysis, the syringe was thermally cleaned with a Hamilton Syringe Cleaner (Model 76610). This analysis was repeated using various fluid volumes of 0.1 to 1.0 μL to calibrate the system's response to each fluid.

To quantify the volume of the absorbed fluid of each analyzed sample, the integrated response of the desorbed compounds was converted into volume by:

$$V_i = R_i f r_i \quad (3.2)$$

where V_i is the volume (μL) of the fluid component i , R_i is the response (area counts) of component i , and $f r_i$ is the response fractor ($\mu\text{L}/\text{area counts}$) of component i obtained from a quadratic regression fit of the fluid calibration. The volume of fluid absorbed was taken as:

$$V_{\text{absorbed}} = \sum_{i=1}^n V_i \quad (3.3)$$

where n is the number of components in the fluid. (Note, the FT and JP-8 fuels were treated as a single component system by integrating the total peak area.)

The volume of the dry solid sample was calculated from the weight of the desorbed polymer (measured on a six-place analytical balance (Metler-Toldeo ModelAX26)) and the density of fluorosilicone (obtained from the D – 471 measurements of the dry source O-ring) as:

$$V_{polymer} = \frac{M_{polymer}}{\rho_{polymer}} \quad (3.4)$$

where $V_{polymer}$ is the volume of the dry polymer (μg), $M_{polymer}$ is the mass of the dry polymer (μg), and $\rho_{polymer}$ is the density of the dry polymer ($\mu\text{g}/\mu\text{L}$). The volume of the dry sample and of the absorbed fluid was then used to estimate the volume fraction of fluid as:

$$V_{fuel} (\%) = \frac{V_{absorbed}}{V_{polymer} + V_{absorbed}} \cdot 100\% \quad (3.5)$$

where V_{fuel} is the volume fraction of absorbed fluid. The volume fraction of the absorbed fluid was then compared with the measured volume swell by D – 471.

CHAPTER IV

RESULTS AND DISCUSSION

The fluorosilicone O-rings were aged in the various test fluids as described earlier. To ensure polymer-fuel equilibrium was reached, one O-ring from each fluid was weighed daily to monitor the progression of the volume swell process. The fuel and polymer were considered to be at equilibrium when the volume ceased to change. Figure 9 displays the mass of absorbed fluid during the immersion period. From this it was determined that the samples approached equilibrium after an exposure time of approximately 200 hours.

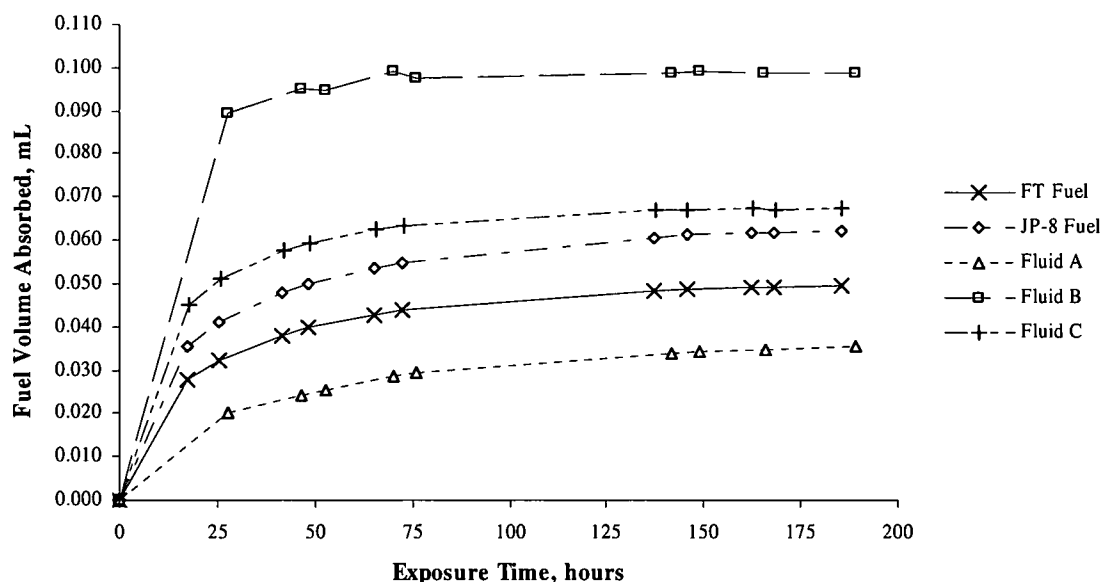


Figure 9. Volume of fuel absorbed by a single O-ring immersed in each fuel by method D-471.

Once the O-ring samples were determined to have reached equilibrium, the volume swell measurements by ASTM method D – 471 for each test fluid were performed as described earlier. The O-rings were then analyzed by the direct thermal desorption GC-MS technique on the STDS system. The volume of the absorbed fluid, volume of the dry polymer and the volume fraction of fluid were determined as mentioned. The volumes of the individual components were added together to obtain the total volume of fuel absorbed. An example of determining the volume of fuel absorbed from the individual species of each fluid is displayed in Table 4 and graphically in Figure 10.

The results on each of the four O-rings for the five test fluids are displayed in Table 5. To quantitatively compare the GC-MS results verses the results from ASTM D – 471, two approaches were used; a two sample *t*-test and paired differences.

Two Sample *t* – Test

To construct a two sample *t*-test, the data for each set of O-rings in each of the five test fluids given in Table 5 were used to calculate the mean and the 90% confidence interval (Student's *t*-distribution) of each fluid. The results of this analysis are shown in Table 6.

Table 4. Fluid component contributions to the volume of fuel absorbed measured by the GC-MS method.

| Fluid | Sample | Fluid Component | Volume Absorbed, μL | Volume Absorbed, % |
|---------|--------------------|---|--------------------------------|--------------------|
| Fluid A | O-ring 1 - Jan1504 | Dodecane Volume (μL) | 0.0420 | 100% |
| | | Total Fuel Volume (μL) | 0.0420 | |
| | | Polymer Volume (μL) | 0.647 | |
| | | Total Volume (μL) | 0.689 | |
| | | Fuel %, v/v | 6.10% | |
| Fluid B | O-ring 1 - Jan2204 | Toluene Volume (μL) | 0.0505 | 54.6% |
| | | Dodecane Volume (μL) | 0.0420 | 45.4% |
| | | Total Fuel Volume (μL) | 0.0925 | |
| | | Polymer Volume (μL) | 0.758 | |
| | | Total Volume (μL) | 0.851 | |
| | | Fuel %, v/v | 10.87% | |
| Fluid C | O-ring 1 - Feb2003 | Decane Volume (μL) | 0.00271 | 9.78% |
| | | Butylcyclohexane Volume (μL) | 0.00235 | 8.48% |
| | | Butylbenzene Volume (μL) | 0.00187 | 6.76% |
| | | Decahydronaphthalene (cis + trans) Volume (μL) | 0.00271 | 9.76% |
| | | Tetrahydronaphthalene Volume (μL) | 0.00442 | 16.0% |
| | | Dodecane Volume (μL) | 0.00499 | 18.0% |
| | | Methylnaphthalene Volume (μL) | 0.00593 | 21.4% |
| | | Tetradecane Volume (μL) | 0.00273 | 9.85% |
| | | Total Fuel Volume (μL) | 0.0277 | |
| | | Polymer Volume (μL) | 0.304 | |
| FT | O-ring 1 - Mar0705 | Total Volume (μL) | 0.332 | |
| | | Fuel %, v/v | 8.35% | |
| | | Total Fuel Volume (μL) | 0.0482 | 100% |
| | | Polymer Volume (μL) | 0.47 | |
| JP-8 | O-ring 1 - Mar0305 | Total Volume (μL) | 0.515 | |
| | | Fuel %, v/v | 9.37% | |
| | | Total Fuel Volume (μL) | 0.0399 | 100% |
| | | Polymer Volume (μL) | 0.471 | |
| | | Total Volume (μL) | 0.511 | |
| | | Fuel %, v/v | 7.81% | |

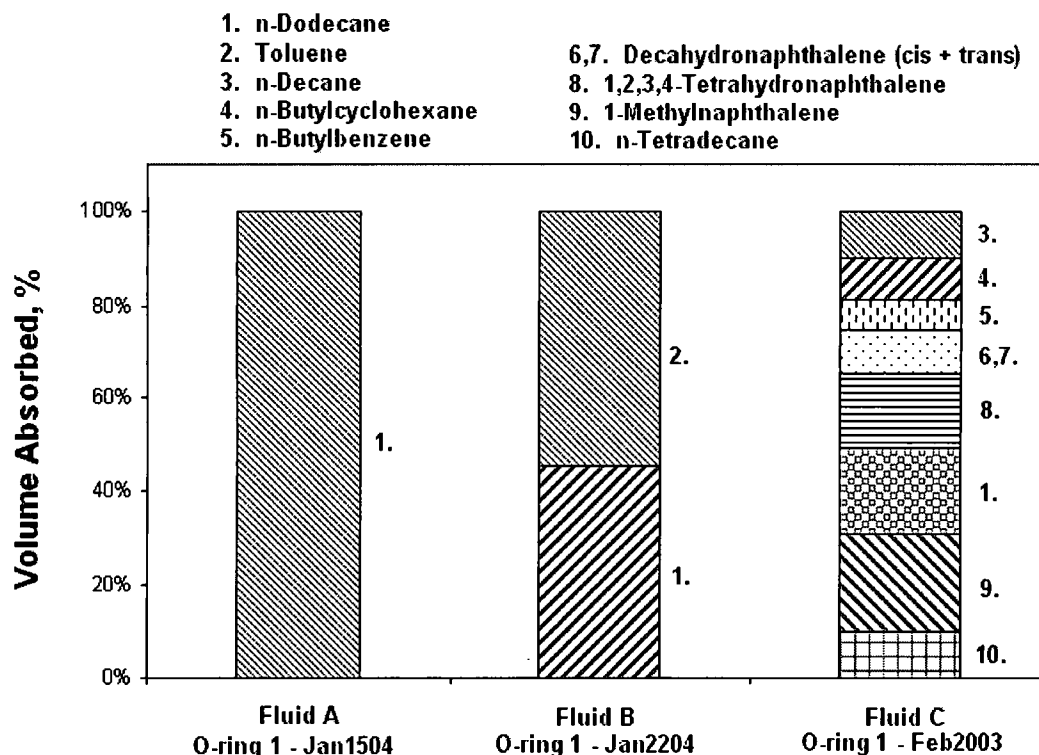


Figure 10. Volume contributions of the absorbed fluid for the individual components of Fluids A, B, and C.

The results show that the volume of fluid absorbed measured by the thermal desorption GC-MS technique exceeded the measured volume swell for Fluids A and C and the FT and JP-8 fuels (Figure 11). Fluid B is the only fluid that displays no difference between the GC-MS and D – 471 measurements at the 90% confidence level. Overall, the two sample *t*-test indicates the volume of fuel absorbed as measured by the direct thermal desorption GC-MS method is approximately 20% greater than the volume swell measured by ASTM D – 471.

Table 5. Individual volume swell of each O-ring by ASTM D – 471 and by direct thermal desorption using a GC-MS.

| Fluid | | Volume Swell by D - 471 | Average Volume Swell by GC-MS |
|---------|----------|-------------------------|-------------------------------|
| Fluid A | O-Ring 1 | 4.53% | 5.73% |
| | O-Ring 2 | 4.71% | 5.09% |
| | O-Ring 3 | 4.41% | 5.98% |
| | O-Ring 4 | 4.38% | 6.00% |
| Fluid B | O-Ring 1 | 12.50% | 10.99% |
| | O-Ring 2 | 12.45% | 11.22% |
| | O-Ring 3 | 11.19% | 11.35% |
| | O-Ring 4 | 11.04% | 11.74% |
| Fluid C | O-Ring 1 | 8.28% | 8.91% |
| | O-Ring 2 | 8.12% | 9.05% |
| | O-Ring 3 | 8.10% | 9.22% |
| | O-Ring 4 | 7.98% | 8.97% |
| FT | O-Ring 1 | 5.74% | 9.49% |
| | O-Ring 2 | 5.83% | 8.17% |
| | O-Ring 3 | 5.77% | 6.76% |
| | O-Ring 4 | 5.63% | 7.45% |
| JP-8 | O-Ring 1 | 7.41% | 8.84% |
| | O-Ring 2 | 7.07% | 9.57% |
| | O-Ring 3 | 7.70% | 9.19% |
| | O-Ring 4 | 7.26% | 9.73% |

Table 6. Volume swell results from the two sample *t*-test on each test fluid.

| Fluid | | ASTM D - 471 | GC-MS | GC-MS / D-471 |
|--|-------------|--------------|-------|---------------|
| Fluid A | Average | 4.51% | 5.70% | 126% |
| | Upper Limit | 4.69% | 6.20% | |
| | Lower Limit | 4.33% | 5.20% | |
| Fluid B | Average | 11.8% | 11.3% | 96.0% |
| | Upper Limit | 12.7% | 11.7% | |
| | Lower Limit | 10.9% | 11.0% | |
| Fluid C | Average | 8.12% | 9.04% | 111% |
| | Upper Limit | 8.27% | 9.20% | |
| | Lower Limit | 7.97% | 8.87% | |
| FT | Average | 5.74% | 7.97% | 139% |
| | Upper Limit | 5.84% | 9.34% | |
| | Lower Limit | 5.65% | 6.59% | |
| JP-8 | Average | 7.36% | 9.33% | 127% |
| | Upper Limit | 7.67% | 9.80% | |
| | Lower Limit | 7.05% | 8.86% | |
| Grand Average of GC-MS compared to D-471 | | | | 120% |

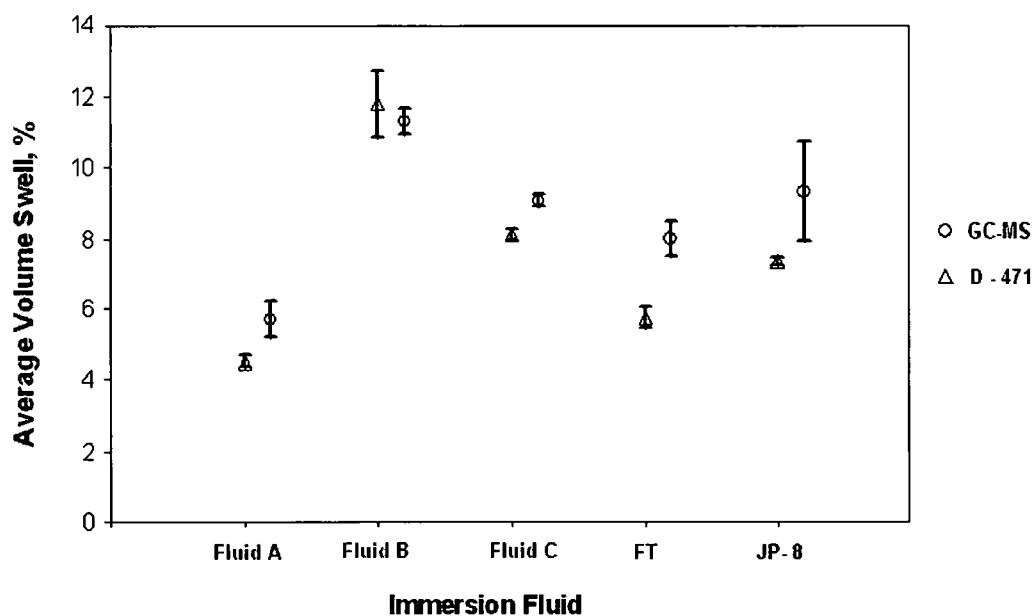


Figure 11. Average volume swell of each test fluid and the 90% confidence intervals.

Paired Difference

The two sample *t*-test summarizes the overall results for each set of O-rings in the individual test fluids. However, since the volume swell by D – 471 and the fuel absorbed measured by the GC-MS technique were obtained for each individual O-ring, the data lends itself to analysis by paired differences. The results of this analysis, as summarized in Table 7 and graphically in Figure 12, from the individual O-rings are consistent with the findings from the two sample *t*-test. Specifically, the volume of absorbed fuel as measured by the GC-MS technique exceeds the volume swell as measured by ASTM D – 471 by a grand average of approximately 20%.

Table 7. Results of paired difference displaying confidence intervals.

| Fluid | | ASTM D - 471 | GC-MS | GC-MS – D-471 | GC-MS / D-471 |
|---------|----------|--------------|----------------------|---------------|---------------|
| Fluid A | O-Ring 1 | 4.53% | 5.73% | 1.20% | 126% |
| | O-Ring 2 | 4.71% | 5.09% | 0.38% | 108% |
| | O-Ring 3 | 4.41% | 5.98% | 1.56% | 135% |
| | O-Ring 4 | 4.38% | 6.00% | 1.62% | 137% |
| | | | Average | 1.19% | 127% |
| | | | Upper Limit | 1.86% | 142% |
| | | | Lower Limit | 0.52% | 111% |
| Fluid B | O-Ring 1 | 12.50% | 10.99% | -1.52% | 88% |
| | O-Ring 2 | 12.45% | 11.22% | -1.23% | 90% |
| | O-Ring 3 | 11.19% | 11.35% | 0.17% | 101% |
| | O-Ring 4 | 11.04% | 11.74% | 0.69% | 106% |
| | | | Average | -0.47% | 96% |
| | | | Upper Limit | 0.79% | 107% |
| | | | Lower Limit | -1.73% | 86% |
| Fluid C | O-Ring 1 | 8.28% | 8.91% | 0.63% | 108% |
| | O-Ring 2 | 8.12% | 9.05% | 0.93% | 111% |
| | O-Ring 3 | 8.10% | 9.22% | 1.12% | 114% |
| | O-Ring 4 | 7.98% | 8.97% | 0.99% | 112% |
| | | | Average | 0.92% | 111% |
| | | | Upper Limit | 1.16% | 114% |
| | | | Lower Limit | 0.68% | 108% |
| FT | O-Ring 1 | 5.74% | 9.49% | 3.76% | 165% |
| | O-Ring 2 | 5.83% | 8.17% | 2.34% | 140% |
| | O-Ring 3 | 5.77% | 6.76% | 0.99% | 117% |
| | O-Ring 4 | 5.63% | 7.45% | 1.82% | 132% |
| | | | Average | 2.23% | 139% |
| | | | Upper Limit | 3.60% | 163% |
| | | | Lower Limit | 0.86% | 115% |
| JP-8 | O-Ring 1 | 7.41% | 8.84% | 1.42% | 119% |
| | O-Ring 2 | 7.07% | 9.57% | 2.49% | 135% |
| | O-Ring 3 | 7.70% | 9.19% | 1.48% | 119% |
| | O-Ring 4 | 7.26% | 9.73% | 2.47% | 134% |
| | | | Average | 1.97% | 127% |
| | | | Upper Limit | 2.67% | 137% |
| | | | Lower Limit | 1.27% | 116% |
| Overall | | | Grand Average | | 120% |
| | | | Upper Limit | | 136% |
| | | | Lower Limit | | 104% |

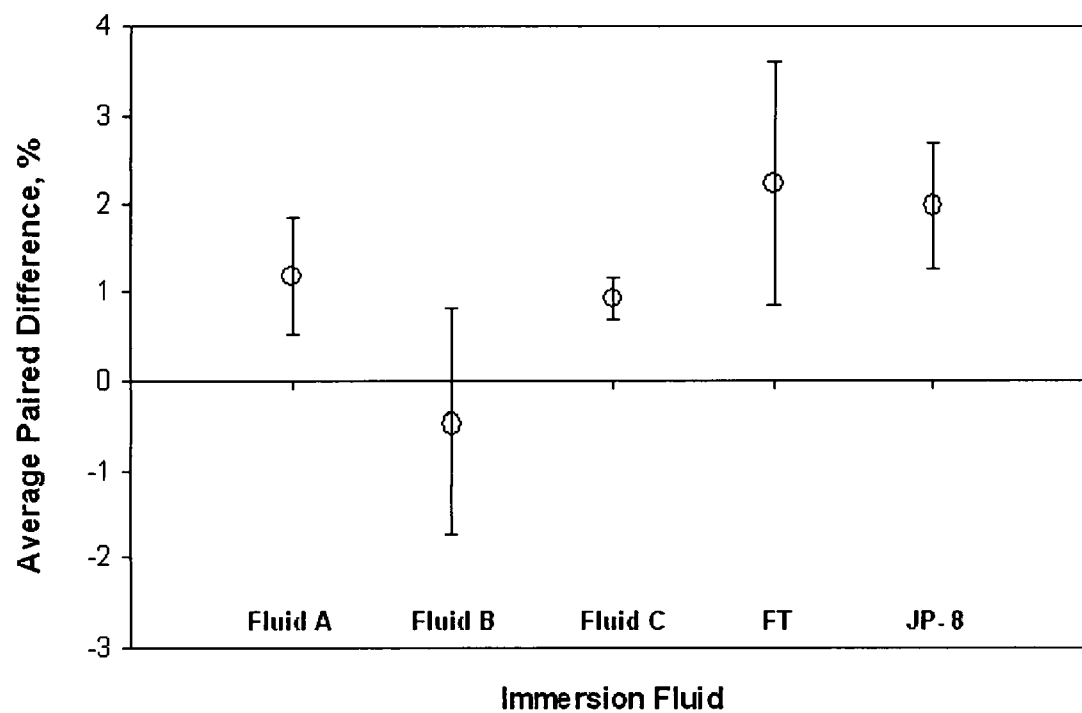


Figure 12. Average paired difference of each test fluid and the 90% confidence intervals.

CHAPTER V

CONCLUSIONS AND RECOMMENDATIONS

Based on the results of this study, it is seen that the GC-MS analysis tends to show more fluid being absorbed than is indicated by the change in volume measured by ASTM D – 471. The relative difference between the two methods, approximately 20%, is significant; however, the absolute difference between the two measurements on each fluid is on the order of 1%. This small difference may be indicative of the free volume of the polymer. Specifically, it is possible for 1% of the absorbed fluid to reside in the free volume and not result in an increase in the overall volume of the sample.

In regards to the past study on nitrile rubber, the large discrepancy between the GC-MS data and the volume swell data was most likely a consequence of the methods being performed under non-equilibrium conditions.²¹ Recent data taken using the two methods and procedures described in this study display a much better relationship between the GC-MS technique and the volume swell (Figure13). This figure demonstrates that with careful liquid calibration and ensuring the samples are at equilibrium, the two methods will be much closer in agreement. Under these conditions, assigning the contributions of various fluid components to the volume swell can be made with better accuracy and confidence.

In the future, analysis should be conducted with careful system calibrations of the chromatographic response for each test fluid. In particular a linear response should not be assumed. Also, the test materials should be aged until equilibrium conditions are present to ensure the samples are at comparable states. Additional data should be taken with a variety of test fluids and O-ring materials to further refine the methods developed in this study.

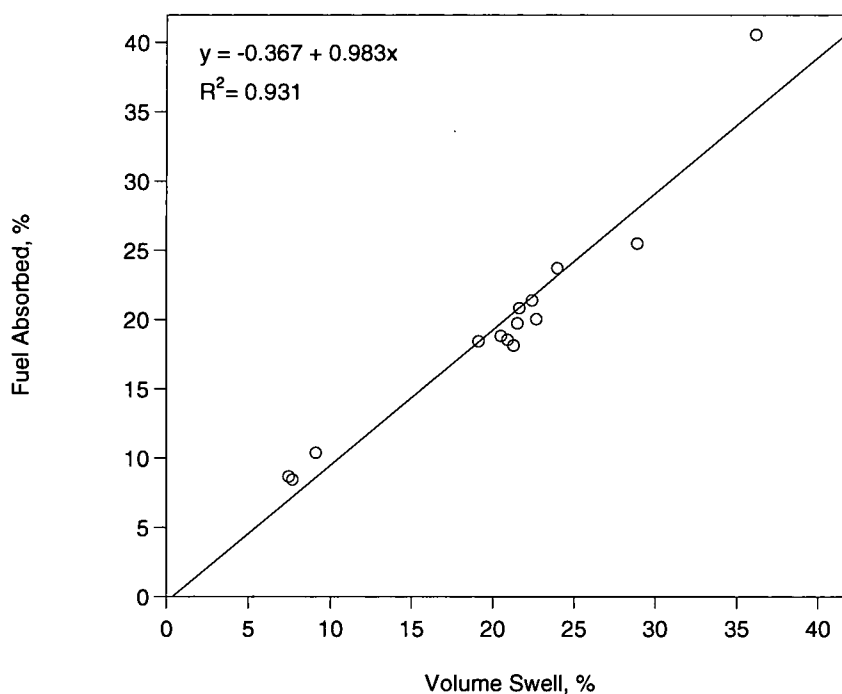
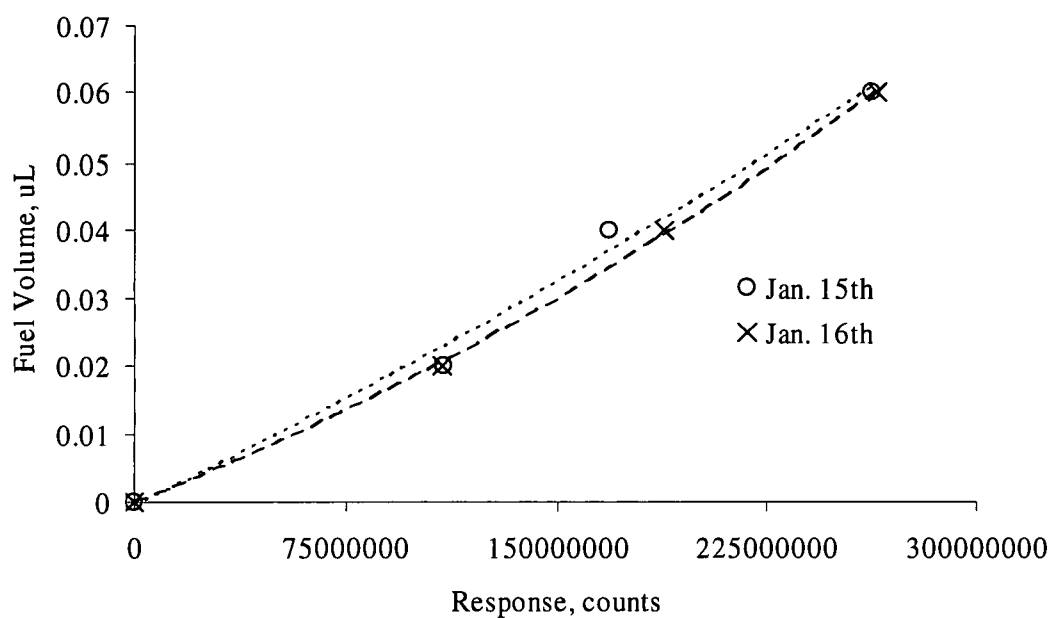


Figure 13. Fuel absorbed versus volume swell for nitrile rubber O-rings aged for 40 hours at room temperature. Prior to aging in fuel the plasticizer had been removed from these O-rings.

APPENDIX

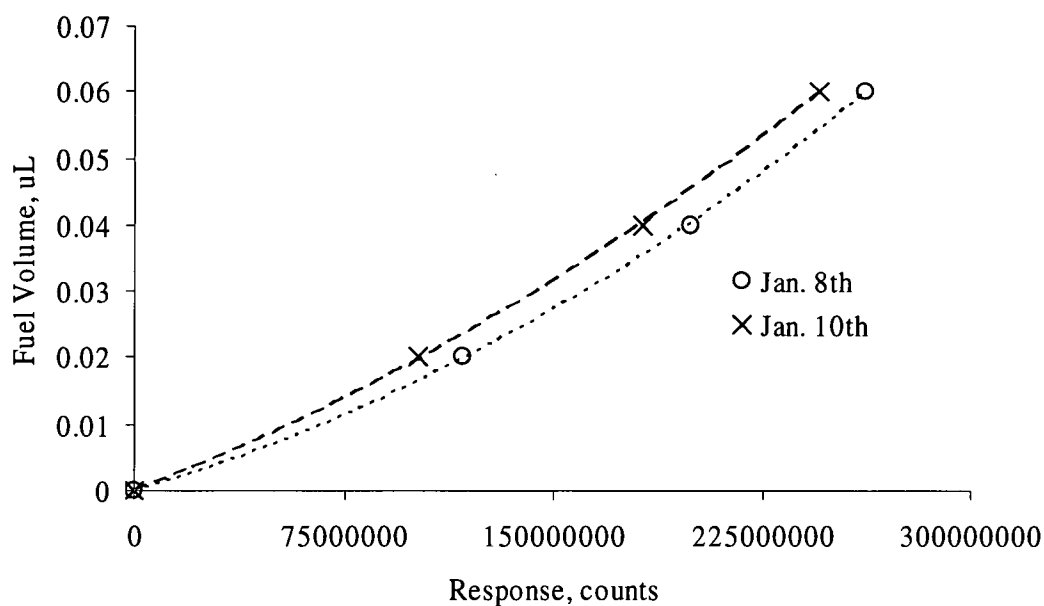
Table A.1. ASTM D – 471 source data measurements.

| Fluid | | Initial Dry Mass, M_1 (g) | Initial Wet Mass, M_2 (g) | Final Dry Mass, M_3 (g) | Final Wet Mass, M_4 (g) |
|---------|----------|-----------------------------|-----------------------------|---------------------------|---------------------------|
| Fluid A | O-Ring 1 | 1.34442 | 0.4802 | 1.37195 | 0.46854 |
| | O-Ring 2 | 1.33114 | 0.47496 | 1.36221 | 0.46569 |
| | O-Ring 3 | 1.34094 | 0.47836 | 1.36882 | 0.46817 |
| | O-Ring 4 | 1.33869 | 0.47771 | 1.36633 | 0.46763 |
| Fluid B | O-Ring 1 | 1.34002 | 0.4784 | 1.42721 | 0.45785 |
| | O-Ring 2 | 1.32787 | 0.47584 | 1.41121 | 0.45307 |
| | O-Ring 3 | 1.33247 | 0.476 | 1.40821 | 0.45592 |
| | O-Ring 4 | 1.33574 | 0.47698 | 1.41091 | 0.45731 |
| Fluid C | O-Ring 1 | 1.32798 | 0.47284 | 1.3838 | 0.46235 |
| | O-Ring 2 | 1.33924 | 0.47671 | 1.39534 | 0.4668 |
| | O-Ring 3 | 1.33776 | 0.47656 | 1.39328 | 0.46673 |
| | O-Ring 4 | 1.33539 | 0.47493 | 1.39094 | 0.46671 |
| FT | O-Ring 1 | 1.33255 | 0.47356 | 1.37027 | 0.46199 |
| | O-Ring 2 | 1.32831 | 0.47284 | 1.36666 | 0.46135 |
| | O-Ring 3 | 1.33901 | 0.4762 | 1.37705 | 0.46448 |
| | O-Ring 4 | 1.34355 | 0.47787 | 1.3811 | 0.46664 |
| JP-8 | O-Ring 1 | 1.34233 | 0.47662 | 1.39327 | 0.46339 |
| | O-Ring 2 | 1.34359 | 0.47768 | 1.38984 | 0.46269 |
| | O-Ring 3 | 1.33962 | 0.47828 | 1.39363 | 0.46594 |
| | O-Ring 4 | 1.3435 | 0.47778 | 1.39391 | 0.46537 |



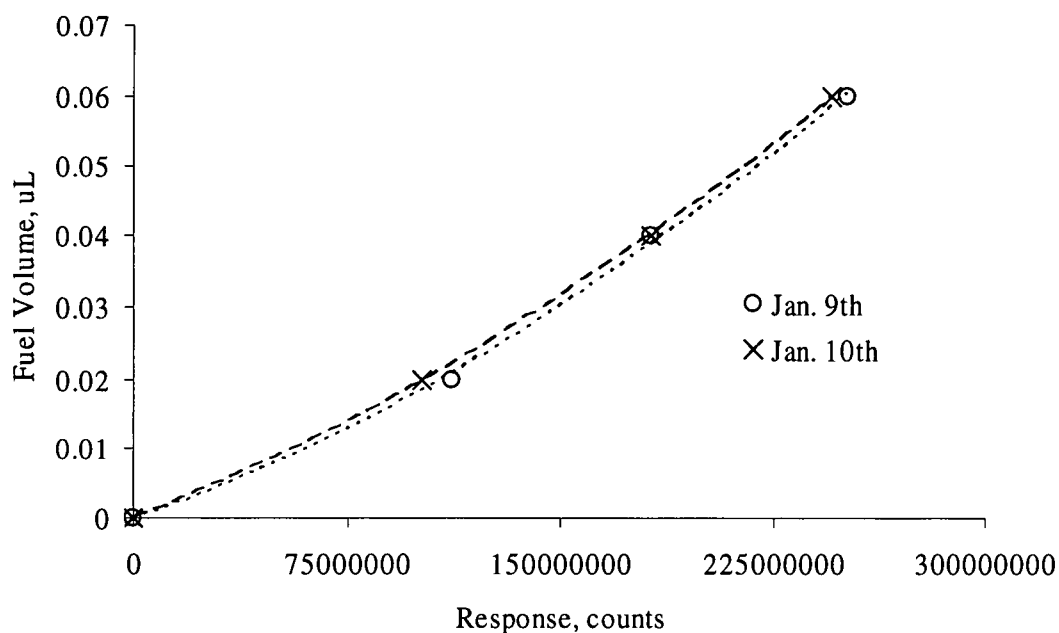
| | JAN1504 | JAN1505 | JAN1506 | JAN1507 |
|--|-----------|-----------|-----------|-----------|
| Mass (ug) | 999 | 1040 | 1263 | 970 |
| Response | 177982349 | 177982349 | 218729332 | 178569227 |
| Fuel Volume Absorbed (uL) | 0.0420 | 0.0441 | 0.0507 | 0.0421 |
| $y = 1.28E-19x^2 + 2.01E-10x - 5.98E-04$ | | | | |
| Poly Volume (uL) | 0.647 | 0.673 | 0.817 | 0.628 |
| Fuel %, v/v | 6.10% | 6.15% | 5.84% | 6.28% |
| | JAN1405 | JAN1406 | JAN1407 | JAN1408 |
| Mass (ug) | 1001 | 1226 | 1440 | 1366 |
| Response | 180968996 | 209386819 | 232203680 | 223173699 |
| Fuel Absorbed (uL) | 0.038 | 0.0455 | 0.0516 | 0.0492 |
| $y = 2.50E-19x^2 + 1.63E-10x - 1.37E-04$ | | | | |
| Poly Volume (uL) | 0.647 | 0.794 | 0.932 | 0.884 |
| Fuel %, v/v | 5.55% | 5.42% | 5.25% | 5.27% |
| Average Fuel %, v/v | 5.73% | | | |

Figure A.1. Calibration curve (above) and calculations (below) for O-ring 1 in Fluid A.



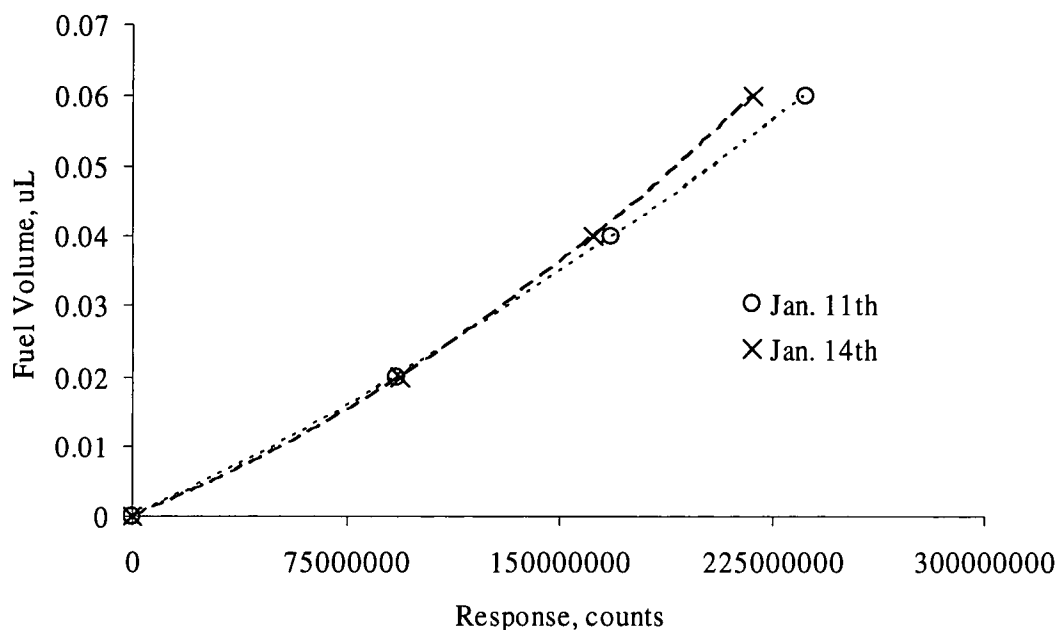
| | JAN0804 | JAN0805 | JAN0806 | JAN0807 | JAN0808 |
|---|--------------------|--------------------|--------------------|--------------------|--------------------|
| Mass (ug) | 1054 | 1547 | 1375 | 1025 | 1297 |
| Response Fuel Volume Absorbed (uL) $y = 4.14E-19x^2 + 1.20E-10x + 4.52E-05$ | 183738540 0.036 | 227678586 0.049 | 208856148 0.043 | 174319559 0.034 | 200064897 0.040 |
| Poly Volume (uL) Fuel %, v/v | 0.683 5.05% | 1.002 4.67% | 0.891 4.62% | 0.664 4.87% | 0.840 4.59% |
| | JAN1004 | JAN1005 | JAN1006 | | |
| Mass (ug) | 1481 | 1681 | 1414 | | |
| Response Fuel Absorbed (uL) $y = 3.47E-19x^2 + 1.59E-10x + 6.50E-05$ | 236636204 0.057 | 257032986 0.064 | 233030409 0.056 | | |
| Poly Volume (uL) Fuel %, v/v | 0.959 5.63% | 1.089 5.53% | 0.916 5.78% | | |
| Average Fuel %, v/v | 5.09% | | | | |

Figure A.2. Calibration curve (above) and calculations (below) for O-ring 2 in Fluid A.



| | JAN0904 | JAN0905 | JAN0906 | JAN0907 | JAN0908 |
|---|---------------------|---------------------|---------------------|--------------------|--------------------|
| Mass (ug) | 1092 | 1205 | 1305 | 1213 | 1273 |
| Response Fuel Volume Absorbed (uL) $y = 3.87E-19x^2 + 1.45E-10x - 1.82E-04$ | 205796617 0.047 | 222494903 0.052 | 230037144 0.054 | 221880256 0.052 | 225659825 0.053 |
| Poly Volume (uL) Fuel %, v/v | 0.707 6.22% | 0.780 6.22% | 0.845 6.01% | 0.786 6.17% | 0.825 6.01% |
| | JAN1004 | JAN1005 | JAN1006 | | |
| Mass (ug) | 1250 | 1486 | 1335 | | |
| Response Fuel Absorbed (uL) $y = 3.47E-19x^2 + 1.59E-10x + 6.50E-05$ | 211232343 0.0493 | 239620991 0.0582 | 221653459 0.0526 | | |
| Poly Volume (uL) Fuel %, v/v | 0.810 5.74% | 0.963 5.70% | 0.865 5.73% | | |
| Average Fuel %, v/v | 5.98% | | | | |

Figure A.3. Calibration curve (above) and calculations (below) for O-ring 3 in Fluid A.



| | JAN1104 | JAN1105 | JAN1106 | JAN1107 |
|---|--------------------|--------------------|--------------------|--------------------|
| Mass (ug) | 1452 | 1074 | 1386 | 1129 |
| Response Fuel Volume Absorbed (uL) $y = 2.53E-19x^2 + 1.95E-10x - 4.80E-05$ | 229927320 0.058 | 180114392 0.044 | 219155816 0.055 | 184614678 0.045 |
| Poly Volume (uL) Fuel %, v/v | 0.998 5.82% | 0.739 5.89% | 0.953 5.77% | 0.776 5.78% |
| | JAN1405 | JAN1406 | JAN1407 | JAN1408 |
| Mass (ug) | 1638 | 945 | 1091 | 1418 |
| Response Fuel Absorbed (uL) $y = 5.04E-19x^2 + 1.66E-10x - 6.28E-06$ | 236308716 0.067 | 164556387 0.041 | 183831429 0.048 | 219082674 0.060 |
| Poly Volume (uL) Fuel %, v/v | 1.127 5.91% | 0.653 6.28% | 0.754 6.35% | 0.979 6.18% |
| Average Fuel %, v/v | 6.00% | | | |

Figure A.4. Calibration curve (above) and calculations (below) for O-ring 4 in Fluid A.

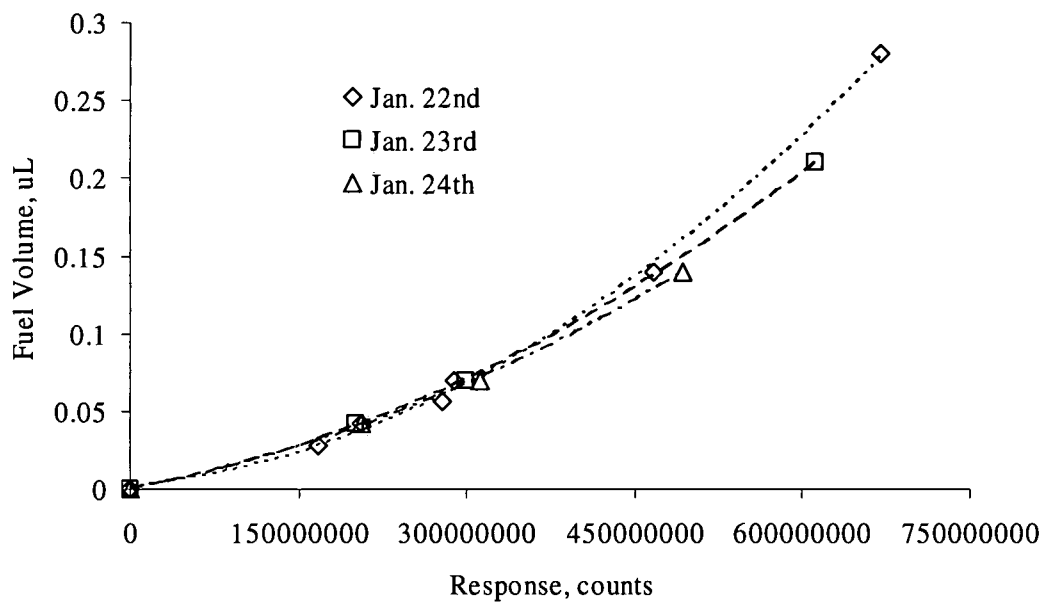
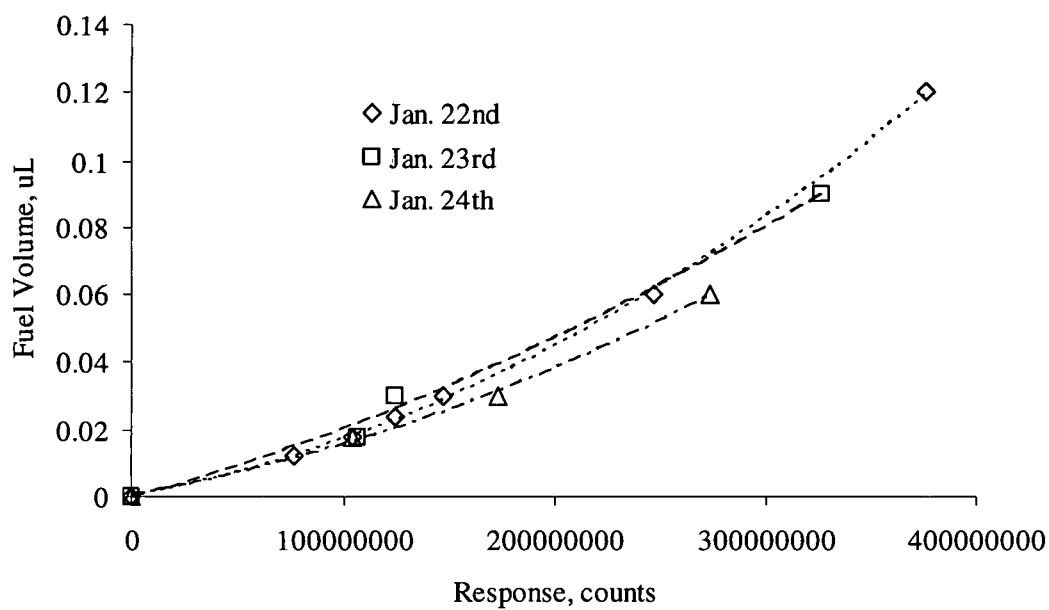


Figure A.5. Calibration curves for Toluene (above) and Dodecane (below) for O-ring 1 in Fluid B.

Table A.2. Calculations for O-ring 1 in Fluid B.

| | JAN2204 | JAN2205 | JAN2206 | JAN2207 | JAN2208 |
|--|-----------|-----------|-----------|-----------|-----------|
| Mass (ug) | 1171 | 2135 | 1194 | 1426 | 1483 |
| Toluene | | | | | |
| Response | 216646989 | 320627196 | 207498208 | 245326670 | 256960282 |
| Fuel Volume Absorbed (uL) | 0.0505 | 0.0925 | 0.0474 | 0.0610 | 0.0654 |
| $y = 5.36E-19x^2 + 1.16E-10x + 2.78E-04$ | | | | | |
| Dodecane | | | | | |
| Response | 220695233 | 317968372 | 214819731 | 240780654 | 252551410 |
| Fuel Absorbed (uL) | 0.0420 | 0.0755 | 0.0403 | 0.0481 | 0.0519 |
| $y = 5.11E-19x^2 + 6.90E-11x + 1.84E-03$ | | | | | |
| Fuel Volume (uL) | 0.092 | 0.168 | 0.088 | 0.109 | 0.117 |
| Poly Volume (uL) | 0.76 | 1.38 | 0.77 | 0.92 | 0.96 |
| Fuel %, v/v | 10.87% | 10.84% | 10.18% | 10.56% | 10.89% |
| | JAN2304 | JAN2305 | JAN2306 | JAN2307 | JAN2308 |
| Mass (ug) | 1215 | 1162 | 1555 | 1133 | 1033 |
| Toluene | | | | | |
| Response | 226935735 | 218305904 | 263356329 | 203327759 | 204503246 |
| Fuel Absorbed (uL) | 0.0555 | 0.0528 | 0.0674 | 0.0482 | 0.0486 |
| $y = 3.09E-19x^2 + 1.76E-10x - 3.80E-04$ | | | | | |
| Dodecane | | | | | |
| Response | 229214174 | 220321115 | 266951898 | 211269516 | 214881752 |
| Fuel Volume Absorbed (uL) | 0.0488 | 0.0462 | 0.0602 | 0.0437 | 0.0447 |
| $y = 3.43E-19x^2 + 1.33E-10x + 2.01E-04$ | | | | | |
| Fuel Volume (uL) | 0.104 | 0.099 | 0.128 | 0.092 | 0.093 |
| Poly Volume (uL) | 0.79 | 0.75 | 1.01 | 0.73 | 0.67 |
| Fuel %, v/v | 11.71% | 11.63% | 11.25% | 11.13% | 12.24% |
| | JAN2404 | JAN2405 | JAN2406 | JAN2407 | |
| Mass (ug) | 851 | 1336 | 1309 | 1132 | |
| Toluene | | | | | |
| Response | 172979622 | 242692643 | 241946445 | 215340604 | |
| Fuel Absorbed (uL) | 0.0315 | 0.0502 | 0.0500 | 0.0424 | |
| $y = 3.67E-19x^2 + 1.16E-10x + 3.82E-04$ | | | | | |
| Dodecane | | | | | |
| Response | 182358644 | 248130353 | 246693655 | 216364371 | |
| Fuel Absorbed (uL) | 0.0348 | 0.0522 | 0.0517 | 0.0435 | |
| $y = 2.99E-19x^2 + 1.35E-10x + 2.70E-04$ | | | | | |
| Fuel Volume (uL) | 0.066 | 0.102 | 0.102 | 0.086 | |
| Poly Volume (uL) | 0.55 | 0.86 | 0.85 | 0.73 | |
| Fuel %, v/v | 10.74% | 10.58% | 10.72% | 10.49% | |
| Average Fuel %, v/v | 10.99% | | | | |

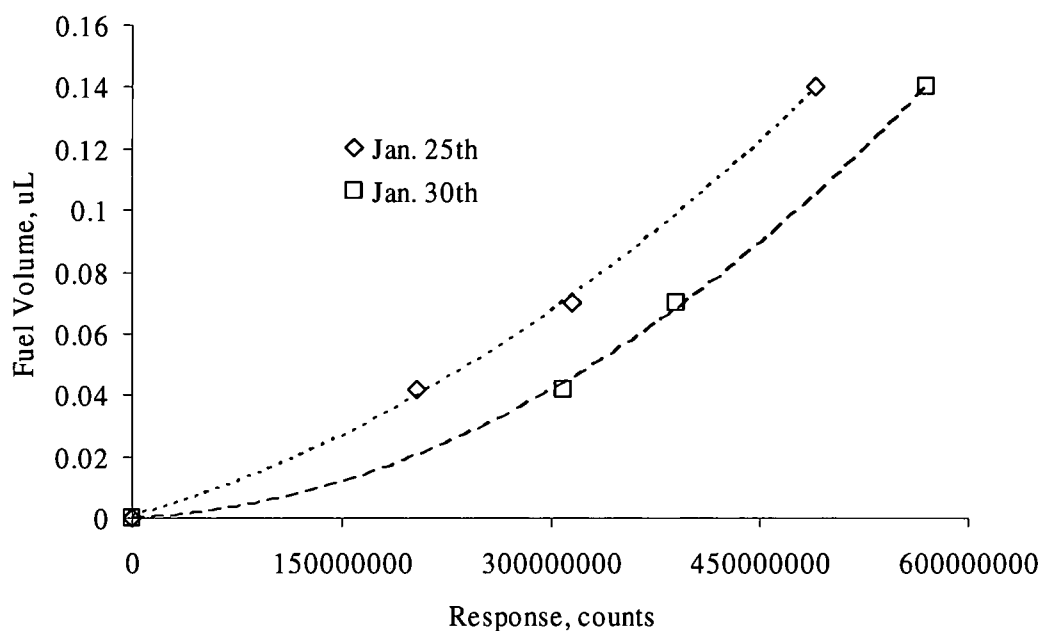
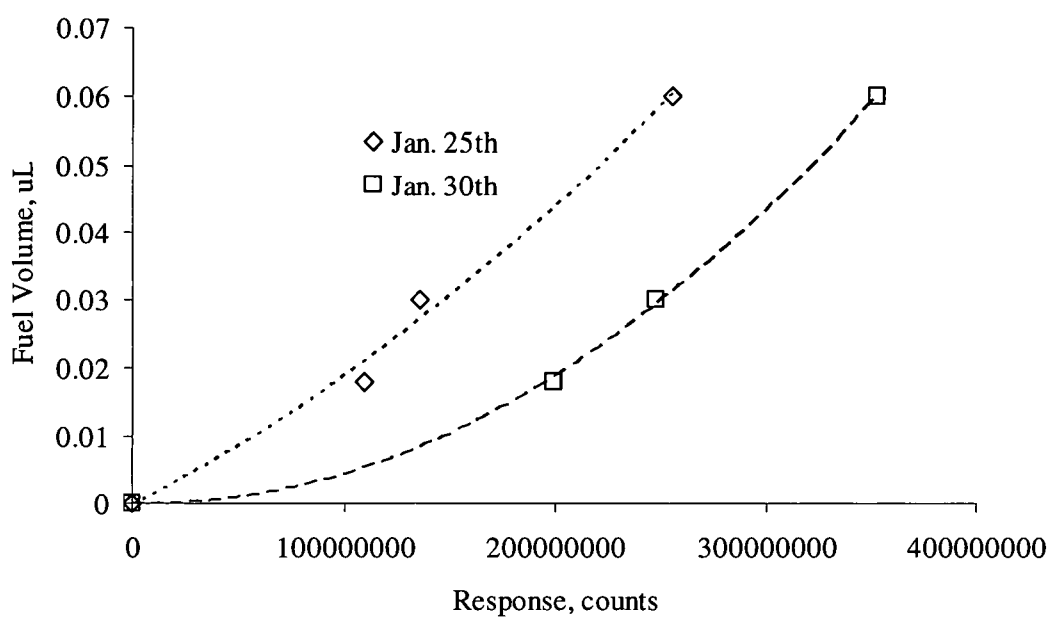


Figure A.6. Calibration curves for Toluene (above) and Dodecane (below) for O-ring 2 in Fluid B.

Table A.3. Calculations for O-ring 2 in Fluid B.

| | JAN2204 | JAN2205 | JAN2206 | JAN2207 | |
|--|-----------|-----------|-----------|-----------|-----------|
| Mass (ug) | 852 | 895 | 1248 | 937 | |
| Toluene | | | | | |
| Response | 165381202 | 185857799 | 230166573 | 188471636 | |
| Fuel Volume Absorbed (uL) | 0.0345 | 0.0400 | 0.0527 | 0.0407 | |
| $y = 3.06E-19x^2 + 1.60E-10x - 3.22E-04$ | | | | | |
| Dodecane | | | | | |
| Response | 183198689 | 185686584 | 240847167 | 186950770 | |
| Fuel Absorbed (uL) | 0.0346 | 0.0352 | 0.0498 | 0.0356 | |
| $y = 3.16E-19x^2 + 1.29E-10x + 4.81E-04$ | | | | | |
| Fuel Volume (uL) | 0.069 | 0.075 | 0.102 | 0.076 | |
| Poly Volume (uL) | 0.55 | 0.58 | 0.81 | 0.61 | |
| Fuel %, v/v | 11.14% | 11.49% | 11.25% | 11.16% | |
| | JAN2304 | JAN2305 | JAN2306 | JAN2307 | JAN2308 |
| Mass (ug) | 995 | 1111 | 579 | 600 | 694 |
| Toluene | | | | | |
| Response | 313698531 | 319556836 | 206651296 | 229868682 | 244467864 |
| Fuel Absorbed (uL) | 0.0475 | 0.0493 | 0.0201 | 0.0251 | 0.0285 |
| $y = 5.02E-19x^2 - 6.09E-12x - 5.19E-05$ | | | | | |
| Dodecane | | | | | |
| Response | 292234018 | 311792723 | 210724578 | 224292386 | 242479071 |
| Fuel Volume Absorbed (uL) | 0.0396 | 0.0446 | 0.0217 | 0.0243 | 0.0280 |
| $y = 3.97E-19x^2 + 1.98E-11x - 1.71E-04$ | | | | | |
| Fuel Volume (uL) | 0.087 | 0.094 | 0.042 | 0.049 | 0.056 |
| Poly Volume (uL) | 0.64 | 0.72 | 0.37 | 0.39 | 0.45 |
| Fuel %, v/v | 11.90% | 11.55% | 10.03% | 11.27% | 11.17% |
| Average Fuel %, v/v | 11.22% | | | | |

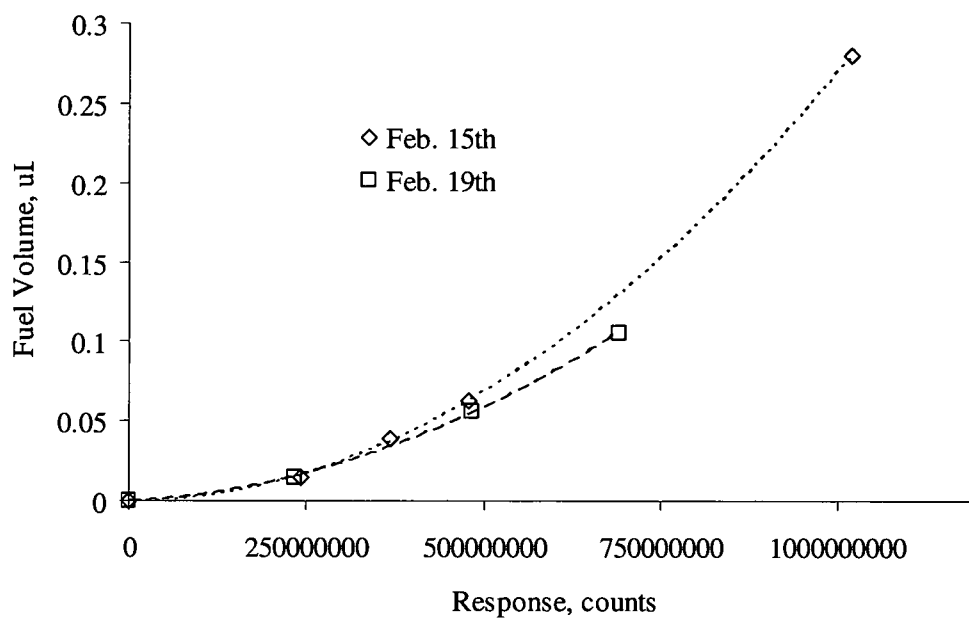
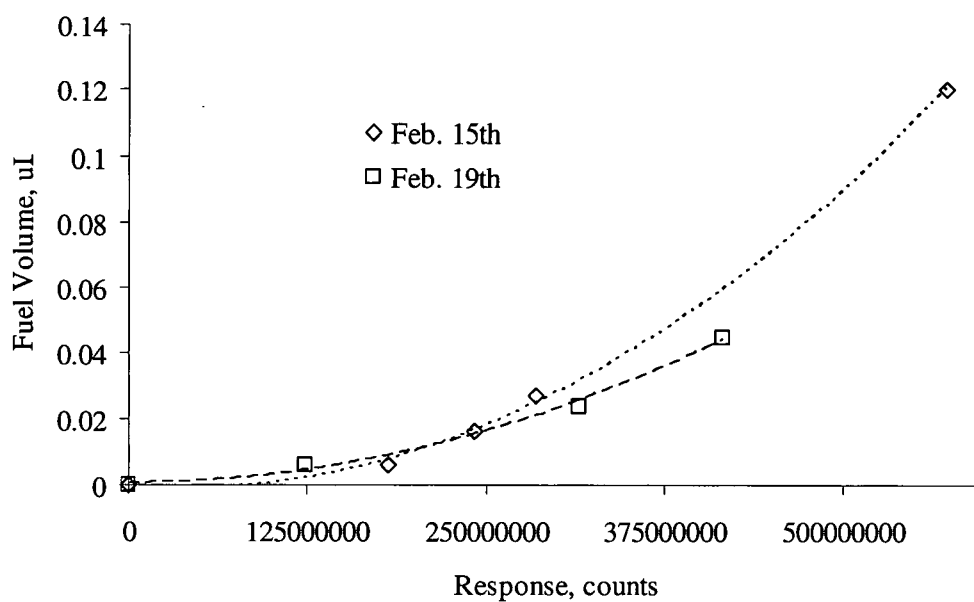


Figure A.7. Calibration curves for Toluene (above) and Dodecane (below) for O-ring 3 in Fluid B.

Table A.4. Calculations for O-ring 3 in Fluid B.

| | JAN1504 | JAN1505 | JAN1506 | JAN1507 |
|---|-------------------------|-------------------------|-------------------------|-------------------------|
| Mass (ug) | 898 | 316 | 530 | 445 |
| Toluene Response Fuel Volume Absorbed (uL) $y = 4.23E-19x^2 - 3.04E-11x - 5.00E-04$ | 353454551 0.0416 | 199653342 0.0103 | 256414442 0.0195 | 232021406 0.0152 |
| Dodecane Response Fuel Absorbed (uL) $y = 2.65E-19x^2 + 5.24E-12x - 5.94E-04$ | 350728593 0.0338 | 260797144 0.0188 | 284035017 0.0223 | 250802471 0.0174 |
| Fuel Volume (uL) Poly Volume (uL) Fuel %, v/v | 0.075 0.58 11.48% | 0.029 0.20 12.44% | 0.042 0.34 10.85% | 0.033 0.29 10.16% |
| | JAN1906 | JAN1907 | | |
| Mass (ug) | 792 | 624 | | |
| Toluene Response Fuel Absorbed (uL) $y = 2.50E-19x^2 + 1.03E-12x + 6.23E-04$ | 325274720 0.0274 | 309092652 0.0264 | | |
| Dodecane Response Fuel Volume Absorbed (uL) $y = 1.90E-19x^2 + 2.27E-11x - 4.29E-04$ | 379318548 0.0354 | 346509104 0.0302 | | |
| Fuel Volume (uL) Poly Volume (uL) Fuel %, v/v | 0.063 0.51 10.92% | 0.057 0.40 12.29% | | |
| Average Fuel %, v/v | 11.35% | | | |

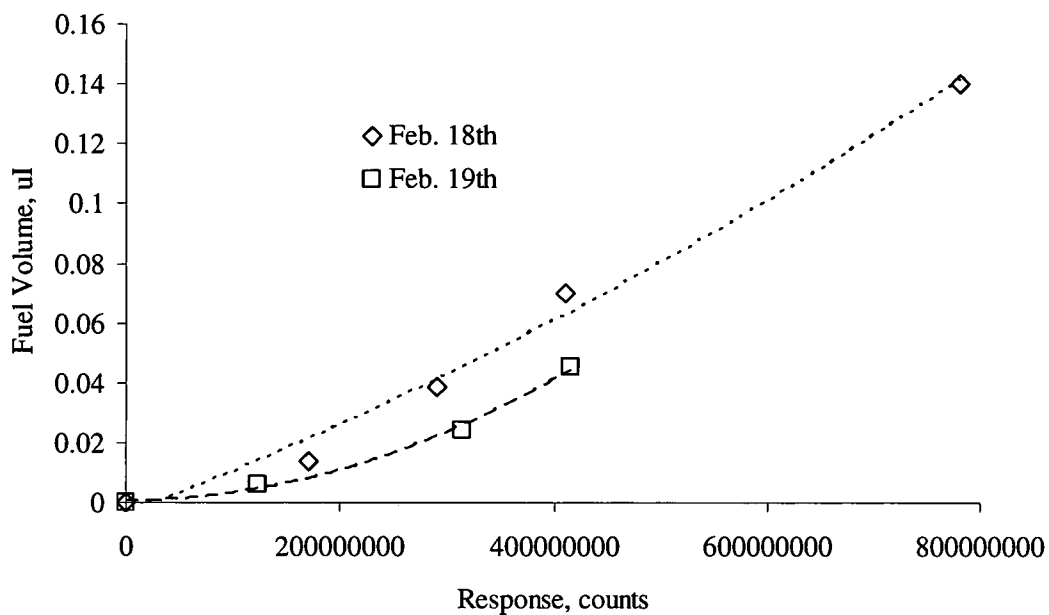
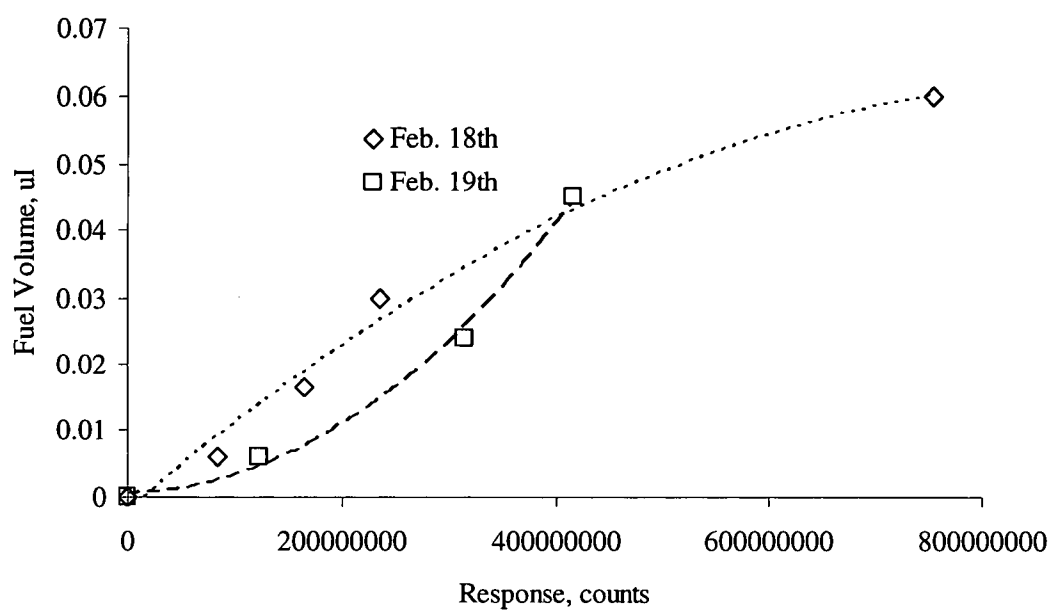


Figure A.8. Calibration curves for Toluene (above) and Dodecane (below) for O-ring 4 in Fluid B.

Table A.5. Calculations for O-ring 4 in Fluid B.

| | FEB1508 | | | |
|---|--------------------------------|--------------------------------|--------------------------------|--------------------------------|
| Mass (ug) | 517 | | | |
| Toluene Response Fuel Absorbed (uL) $y = 2.50E-19x^2 + 1.03E-12x + 6.23E-04$ | 243944594 0.0172 | | | |
| Dodecane Response Fuel Volume Absorbed (uL) $y = 1.90E-19x^2 + 2.27E-11x - 4.29E-04$ | 269957640 0.0201 | | | |
| Fuel Volume (uL) Poly Volume (uL) Fuel %, v/v | 0.037 0.33 10.04% | | | |
| | FEB1806 | FEB1807 | FEB1808 | |
| Mass (ug) | 444 | 376 | 970 | |
| Toluene Response Fuel Volume Absorbed (uL) $y = -7.71E-20x^2 + 1.41E-10x - 2.29E-03$ | 180146565 0.0152 | 165371481 0.0127 | 304165368 0.0446 | |
| Dodecane Response Fuel Absorbed (uL) $y = 6.46E-20x^2 + 1.35E-10x - 3.75E-03$ | 212783535 0.0220 | 194741569 0.0188 | 328782010 0.0493 | |
| Fuel Volume (uL) Poly Volume (uL) Fuel %, v/v | 0.037 0.29 11.46% | 0.031 0.24 11.44% | 0.094 0.63 13.00% | |
| | FEB1904 | FEB1905 | FEB1909 | FEB1910 |
| Mass (ug) | 543 | 839 | 675 | 627 |
| Toluene Response Fuel Absorbed (uL) $y = 2.50E-19x^2 + 1.03E-12x + 6.23E-04$ | 279886802 0.0205 | 366101506 0.0345 | 331782065 0.0285 | 312342020 0.0253 |
| Dodecane Response Fuel Volume Absorbed (uL) $y = 1.90E-19x^2 + 2.27E-11x - 4.29E-04$ | 313449981 0.0253 | 400605513 0.0391 | 362710917 0.0327 | 352895503 0.0312 |
| Fuel Volume (uL) Poly Volume (uL) Fuel %, v/v | 0.046 0.35 11.52% | 0.074 0.54 11.93% | 0.061 0.44 12.28% | 0.057 0.41 12.22% |
| Average Fuel %, v/v | 11.74% | | | |

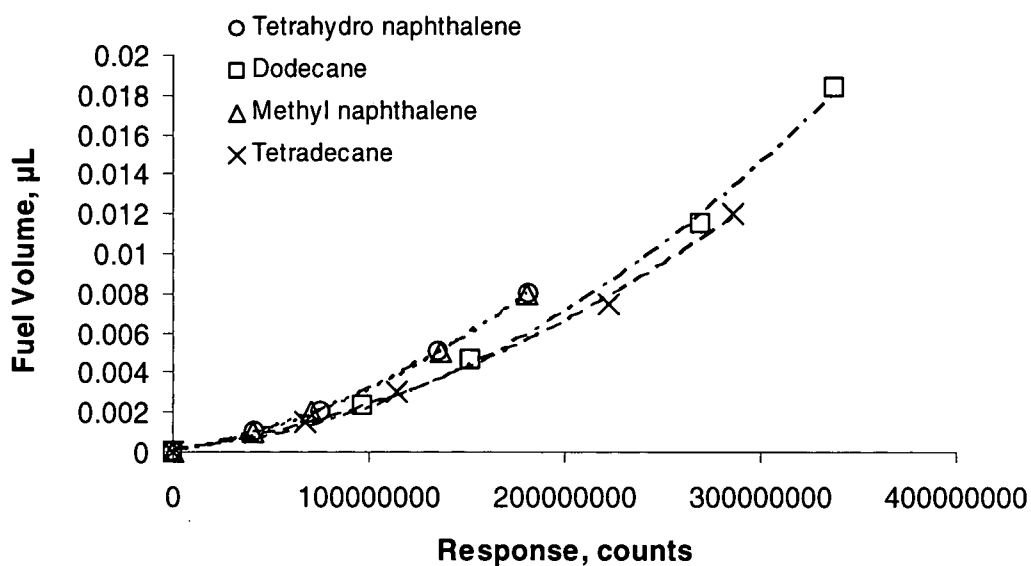
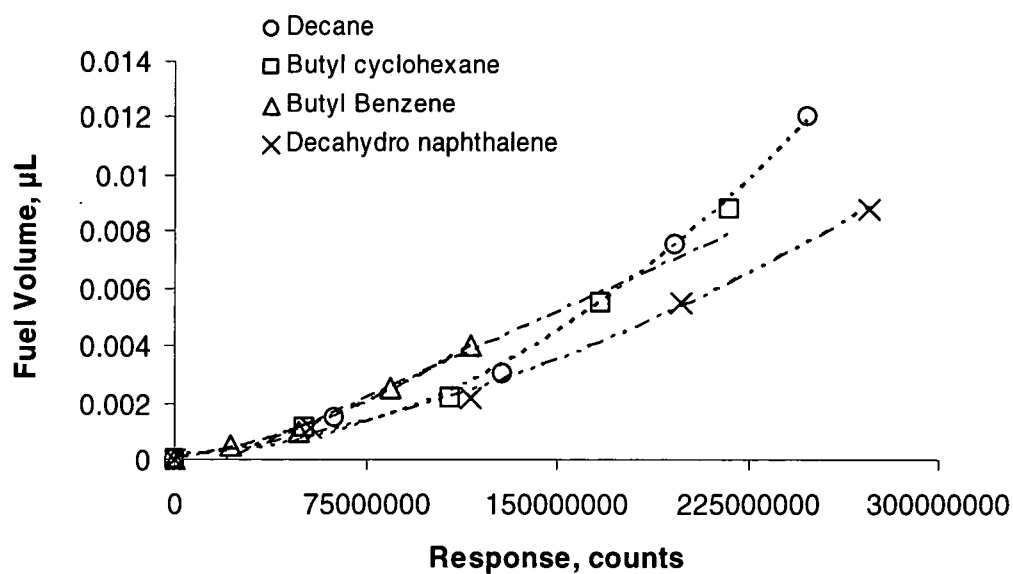


Figure A.9. Fluid C component calibration curves for O-ring 1.

Table A.6. Calculations for O-ring 1 for Fluid C.

| | FEB2003 | FEB2004 | FEB2005 | FEB2006 | FEB2007 | FEB2010 |
|---|---------------------------|---------------------------|---------------------------|---------------------------|---------------------------|---------------------------|
| Polymer Weight (ug) | 470 | 656 | 407 | 845 | 885 | 550 |
| Decane (1) Response Volume Absorbed (uL) $y = 1.88E-19x^2 + 2.65E-13x + 2.09E-04$ | 114519511 0.0027 | 167053621 0.0055 | 100624835 0.0021 | 180445281 0.0064 | 189857101 0.0071 | 130908732 0.0035 |
| Butylcyclohexane (2) Response Volume Absorbed (uL) $y = 1.64E-19x^2 + 4.18E-12x + 1.26E-04$ | 104423779 0.0023 | 152910198 0.0046 | 92325191 0.0019 | 166340306 0.0054 | 174557082 0.0058 | 119664078 0.0030 |
| Butyl Benzene (3) Response Volume Absorbed (uL) $y = 1.84E-19x^2 + 1.28E-11x + 3.21E-05$ | 71184613 0.0019 | 102279413 0.0033 | 61741837 0.0015 | 116282533 0.0040 | 123097866 0.0044 | 82429024 0.0023 |
| Decahydronaphthalene (4 + 5) (cis + trans) Response Volume Absorbed (uL) $y = 7.55E-20x^2 + 1.16E-11x + 6.25E-05$ | 125382814 0.0027 | 187247587 0.0049 | 108631303 0.0022 | 210602623 0.0059 | 222922238 0.0064 | 144462474 0.0033 |
| Tetrahydronaphthalene (6) Response Volume Absorbed (uL) $y = 1.60E-19x^2 + 1.47E-11x + 2.56E-05$ | 126005391 0.0044 | 163653460 0.0067 | 110872431 0.0036 | 187656265 0.0084 | 195177503 0.0090 | 140691813 0.0053 |
| Dodecane (7) Response Volume Absorbed (uL) $y = 1.35E-19x^2 + 7.84E-12x + 1.15E-04$ | 163413200 0.0050 | 210994120 0.0078 | 145537950 0.0041 | 246427850 0.0102 | 257064755 0.0110 | 183029878 0.0061 |
| Methyl Naphthalene (8) Response Volume Absorbed (uL) $y = 1.50E-19x^2 + 1.67E-11x + 3.18E-05$ | 150299876 0.0059 | 183332461 0.0081 | 136783863 0.0051 | 212387150 0.0103 | 218639456 0.0109 | 165037252 0.0069 |
| Tetradecane (9) Response Volume Absorbed (uL) $y = 9.85E-20x^2 + 1.29E-11x + 9.43E-05$ | 110727183 0.0027 | 146205690 0.0041 | 100392372 0.0024 | 181383095 0.0057 | 183657581 0.0058 | 126797922 0.0033 |
| Fuel Volume (uL) Poly Volume (uL) Fuel %, v/v | 0.0277 0.3043 8.35% | 0.0450 0.4247 9.57% | 0.0230 0.2635 8.04% | 0.0563 0.5471 9.33% | 0.0604 0.5730 9.53% | 0.0336 0.3561 8.63% |
| Average Fuel %, v/v | 8.91% | | | | | |

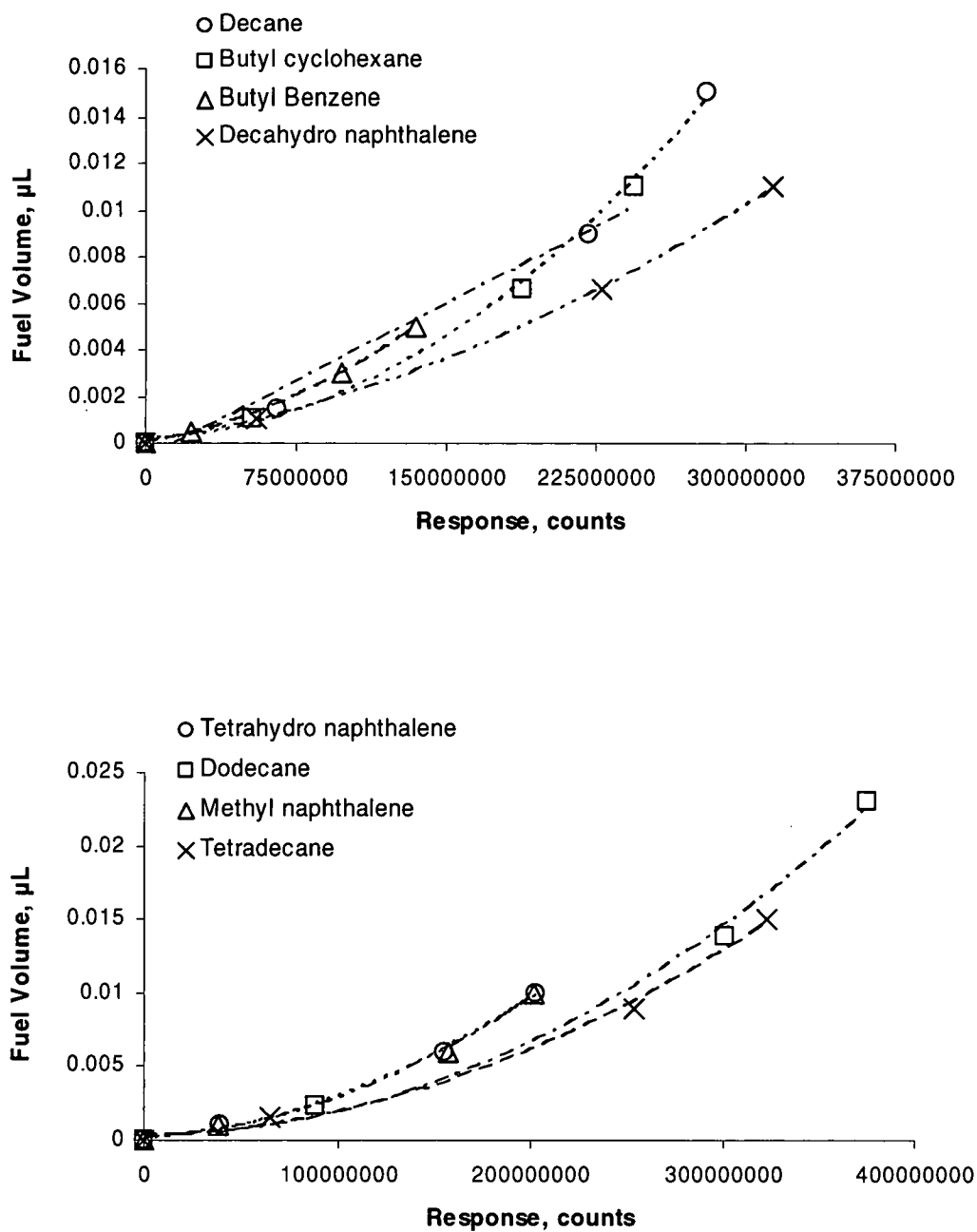


Figure A.10. Fluid C component calibration curves for O-ring 2.

Table A.7. Calculations for O-ring 2 for Fluid C.

| | FEB2104 | FEB2105 | FEB2106 | FEB2107 | FEB2108 | FEB2109 |
|---|---------------------------|---------------------------|---------------------------|---------------------------|---------------------------|---------------------------|
| Polymer Weight (ug) | 762 | 635 | 762 | 566 | 753 | 665 |
| Decane (1) Response Fuel Absorbed (uL) $y = 1.74E-19x^2 + 3.07E-12x + 1.97E-04$ | 165088831 0.0055 | 135950016 0.0038 | 171157785 0.0058 | 146626024 0.0044 | 177116424 0.0062 | 153854856 0.0048 |
| Butylcyclohexane (2) Response Volume Absorbed (uL) $y = 1.53E-19x^2 + 6.88E-12x + 1.10E-04$ | 152211594 0.0047 | 125656868 0.0034 | 155018415 0.0049 | 130829677 0.0036 | 158992811 0.0051 | 138611465 0.0040 |
| Butyl Benzene (3) Response Volume Absorbed (uL) $y = 1.60E-19x^2 + 1.49E-11x + 3.13E-05$ | 106288176 0.0034 | 84984663 0.0025 | 109847208 0.0036 | 91121891 0.0027 | 113069405 0.0038 | 97578340 0.0030 |
| Decahydronaphthalene (4 + 5) (cis + trans) Response Volume Absorbed (uL) $y = 6.84E-20x^2 + 1.34E-11x + 5.85E-05$ | 189756020 0.0051 | 154380363 0.0038 | 194276090 0.0052 | 160186217 0.0040 | 199176106 0.0054 | 170751742 0.0043 |
| Tetrahydronaphthalene (6) Response Volume Absorbed (uL) $y = 1.92E-19x^2 + 9.16E-12x + 1.25E-04$ | 176293214 0.0077 | 147652500 0.0057 | 177042353 0.0078 | 150810305 0.0059 | 179156148 0.0079 | 159671501 0.0065 |
| Dodecane (7) Response Volume Absorbed (uL) $y = 1.59E-19x^2 - 6.15E-13x + 3.86E-04$ | 233701238 0.0089 | 194857377 0.0063 | 228059019 0.0085 | 197837604 0.0065 | 232515896 0.0088 | 207132933 0.0071 |
| Methyl Naphthalene (8) Response Volume Absorbed (uL) $y = 2.06E-19x^2 + 6.20E-12x + 1.69E-04$ | 203149618 0.0099 | 180584086 0.0080 | 200331635 0.0097 | 172625805 0.0074 | 202851331 0.0099 | 187056681 0.0086 |
| Tetradecane (9) Response Volume Absorbed (uL) $y = 1.26E-19x^2 + 4.02E-12x + 2.63E-04$ | 169215606 0.0046 | 141018693 0.0033 | 161223973 0.0042 | 135051705 0.0031 | 166860251 0.0045 | 150015848 0.0037 |
| Fuel Volume (uL) Poly Volume (uL) Fuel %, v/v | 0.0498 0.4934 9.17% | 0.0368 0.4111 8.21% | 0.0497 0.4934 9.15% | 0.0376 0.3665 9.30% | 0.0516 0.4875 9.58% | 0.0420 0.4305 8.88% |
| Average Fuel %, v/v | 9.05% | | | | | |

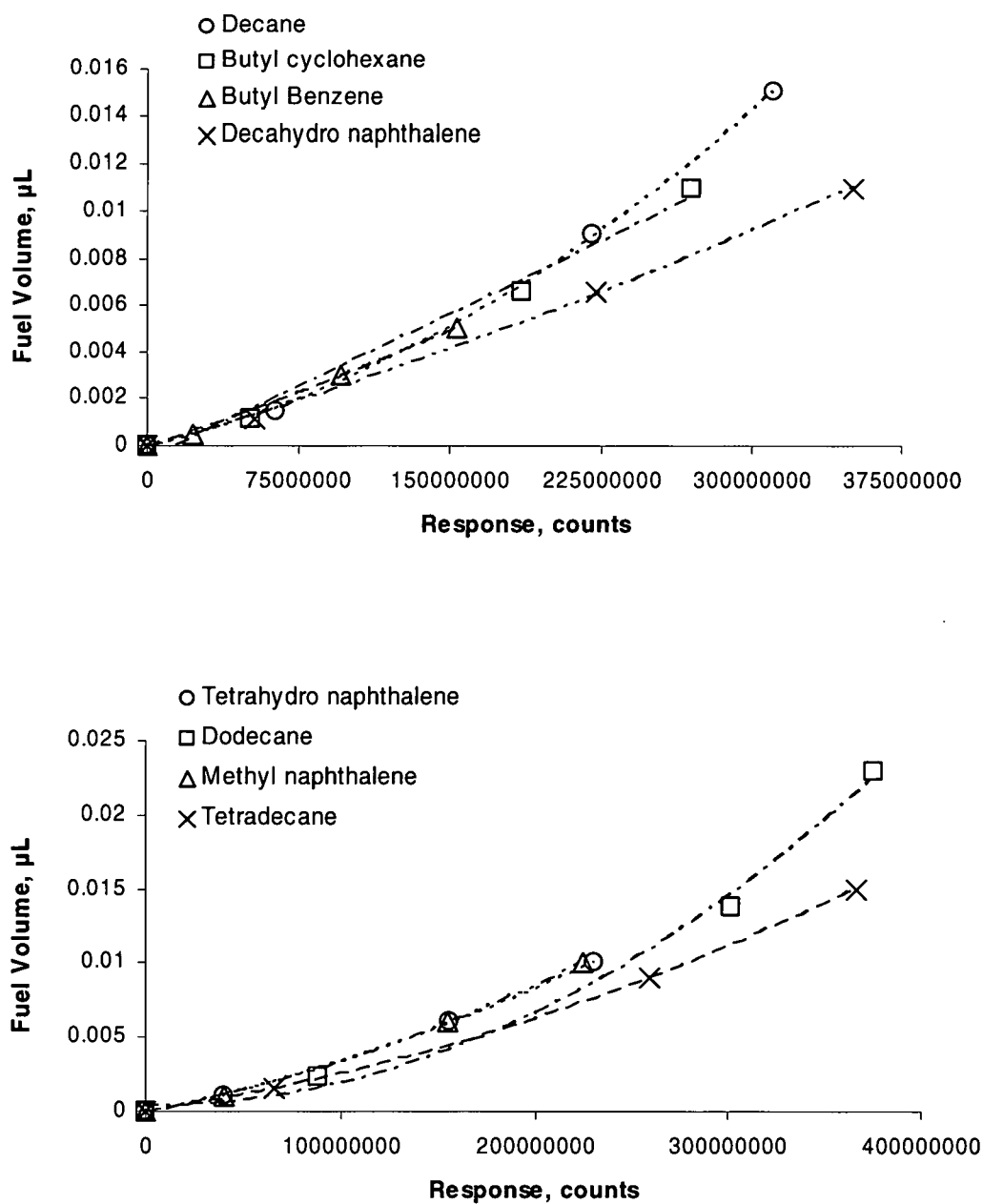


Figure A.11. Fluid C component calibration curves for O-ring 3.

Table A.8. Calculations for O-ring 3 for Fluid C.

| | FEB2605 | FEB2606 | FEB2607 | FEB2608 | FEB2609 | FEB2610 |
|---|---------------------------|---------------------------|---------------------------|---------------------------|---------------------------|---------------------------|
| Polymer Weight (ug) | 539 | 444 | 631 | 356 | 738 | 475 |
| Decane (1) Response Volume Absorbed (uL) $y = 8.86E-20x^2 + 2.11E-11x - 7.60E-05$ | 131079739 0.0042 | 113092582 0.0034 | 146457148 0.0049 | 92417149 0.0026 | 183380401 0.0068 | 117530340 0.0036 |
| Butylcyclohexane (2) Response Volume Absorbed (uL) $y = 6.98E-20x^2 + 2.24E-11x - 8.35E-05$ | 118553860 0.0036 | 102090096 0.0029 | 132523432 0.0041 | 83567351 0.0023 | 163545408 0.0054 | 106010854 0.0031 |
| Butyl Benzene (3) Response Volume Absorbed (uL) $y = 3.08E-20x^2 + 2.85E-11x - 5.92E-05$ | 81552737 0.0025 | 69796458 0.0021 | 92970559 0.0029 | 56255561 0.0016 | 113254133 0.0036 | 73436093 0.0022 |
| Decahydronaphthalene (4 + 5) (cis + trans) Response Volume Absorbed (uL) $y = 1.75E-20x^2 + 2.58E-11x - 1.27E-04$ | 144266491 0.0040 | 121613271 0.0033 | 163487860 0.0046 | 97516912 0.0026 | 203273220 0.0058 | 127001880 0.0034 |
| Tetrahydronaphthalene (6) Response Fuel Absorbed (uL) $y = 7.33E-20x^2 + 2.69E-11x - 7.19E-05$ | 143980651 0.0053 | 125917710 0.0045 | 141318857 0.0052 | 103795700 0.0035 | 180486903 0.0072 | 129272415 0.0046 |
| Dodecane (7) Response Volume Absorbed (uL) $y = 9.29E-20x^2 + 1.53E-11x + 3.02E-04$ | 194367963 0.0065 | 170201431 0.0053 | 187615985 0.0062 | 137102801 0.0039 | 232398640 0.0086 | 168194824 0.0052 |
| Methyl Naphthalene (8) Response Volume Absorbed (uL) $y = 9.00E-20x^2 + 2.46E-11x - 5.23E-05$ | 170532479 0.0068 | 150175915 0.0057 | 168475450 0.0066 | 126565778 0.0045 | 199533866 0.0084 | 154104301 0.0059 |
| Tetradecane (9) Response Volume Absorbed (uL) $y = 5.90E-20x^2 + 1.94E-11x - 1.61E-05$ | 131129880 0.0035 | 115466523 0.0030 | 130298271 0.0035 | 92465145 0.0023 | 162967215 0.0047 | 114344868 0.0030 |
| Fuel Volume (uL) Poly Volume (uL) Fuel %, v/v | 0.0363 0.3490 9.43% | 0.0302 0.2875 9.51% | 0.0380 0.4085 8.50% | 0.0233 0.2305 9.17% | 0.0505 0.4778 9.57% | 0.0310 0.3075 9.17% |
| Average Fuel %, v/v | 9.22% | | | | | |

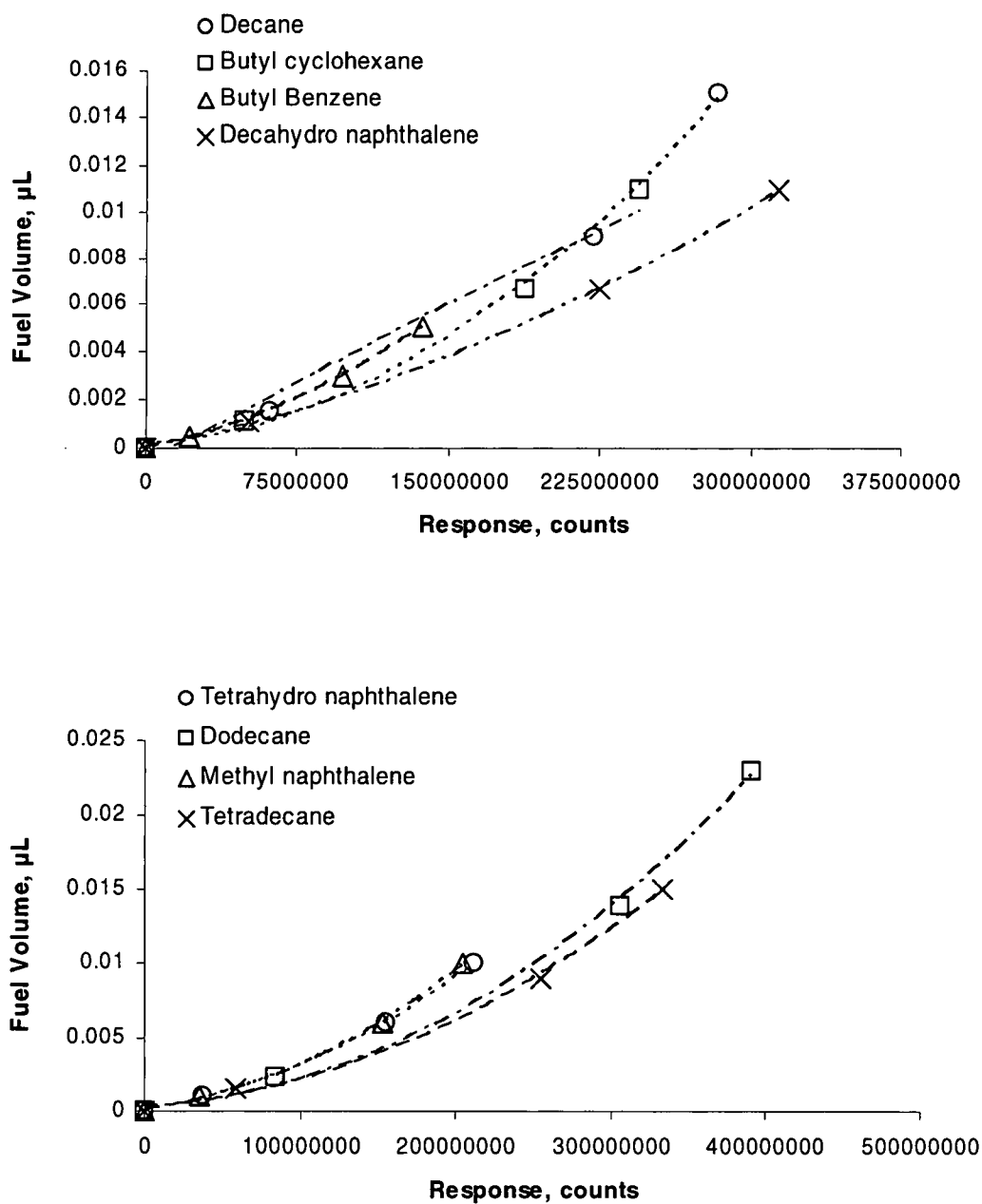
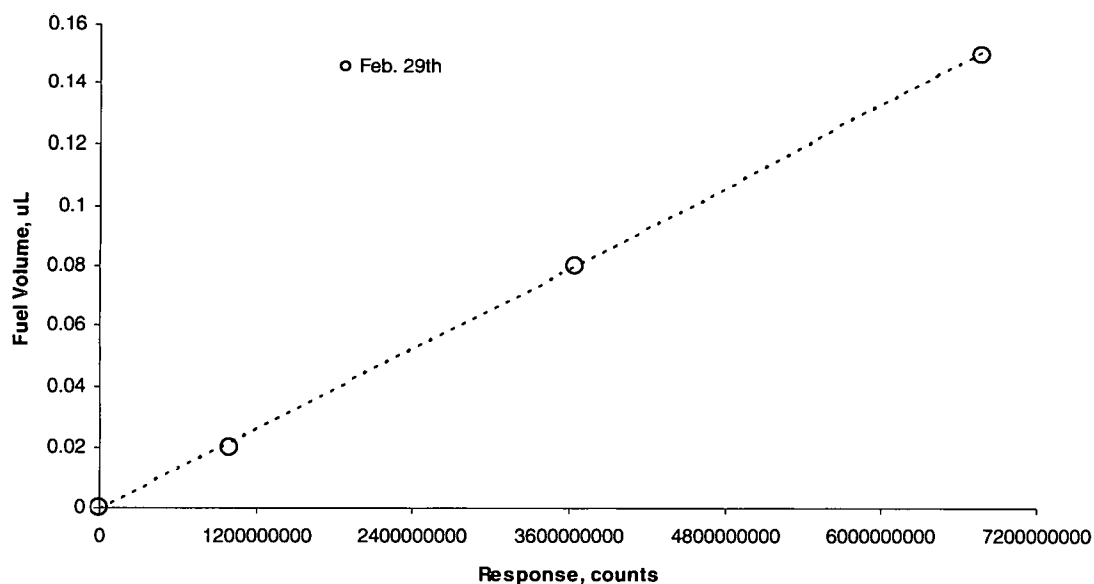


Figure A.12. Fluid C. component calibration curves for O-ring 4.

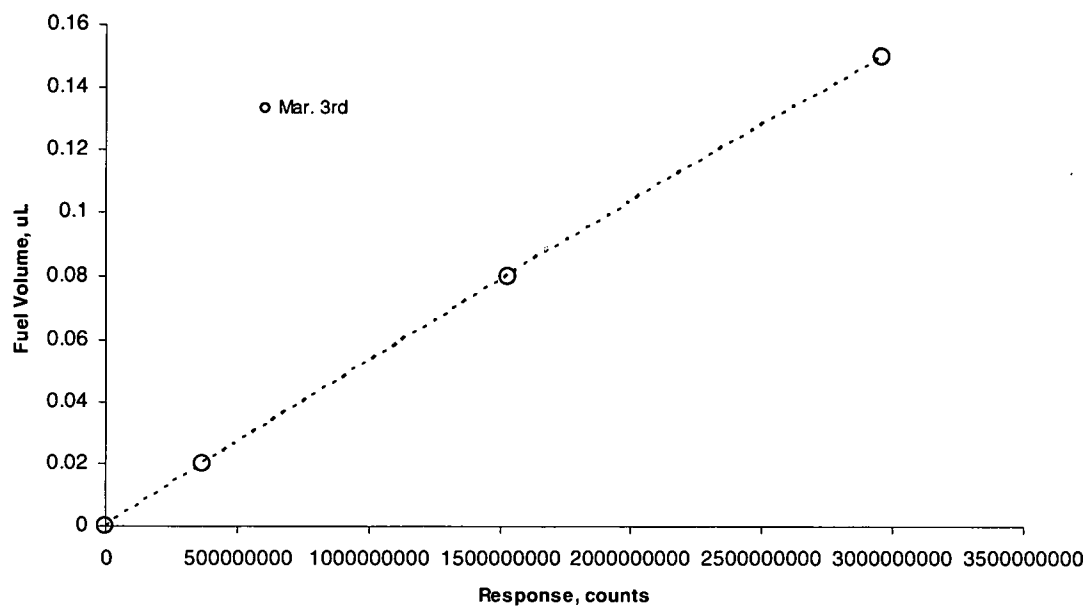
Table A.9. Calculations for O-ring 4 for Fluid C.

| | FEB2705 | FEB2706 | FEB2707 | FEB2708 | FEB2709 | FEB2710 |
|---|---------------------------|---------------------------|---------------------------|---------------------------|---------------------------|----------------------------|
| Polymer Weight (ug) | 532 | 586 | 449 | 818 | 667 | 380 |
| Decane (1) Response Volume Absorbed (uL) $y = 1.64E-19x^2 + 4.94E-12x + 2.09E-04$ | 126630980 0.0035 | 139482925 0.0041 | 111342624 0.0028 | 181022791 0.0065 | 157941213 0.0051 | 94098794 0.0021 |
| Butylcyclohexane (2) Response Volume Absorbed (uL) $y = 1.50E-19x^2 + 7.39E-12x + 1.37E-04$ | 114739972 0.0030 | 126226133 0.0035 | 99453307 0.0024 | 164680583 0.0054 | 127833605 0.0035 | 84362611 0.0018 |
| Butyl Benzene (3) Response Volume Absorbed (uL) $y = 1.38E-19x^2 + 1.73E-11x + 2.44E-05$ | 79828310 0.0023 | 88837384 0.0027 | 69010527 0.0019 | 117571616 0.0040 | 102801019 0.0033 | 59491331 0.0015 |
| Decahydronaphthalene (4 + 5) (cis + trans) Response Volume Absorbed (uL) $y = 6.09E-20x^2 + 1.58E-11x + 5.31E-05$ | 139811375 0.0034 | 153670358 0.0039 | 118523888 0.0028 | 206159483 0.0059 | 153916298 0.0039 | 104276030 0.0024 |
| Tetrahydronaphthalene (6) Response Volume Absorbed (uL) $y = 1.43E-19x^2 + 1.64E-11x + 6.95E-05$ | 141679389 0.0053 | 152101874 0.0059 | 123152914 0.0043 | 190291581 0.0084 | 160524552 0.0064 | 110547719 0.0036 |
| Dodecane (7) Response Volume Absorbed (uL) $y = 1.33E-19x^2 + 5.12E-12x + 3.36E-04$ | 188740046 0.0060 | 197083384 0.0065 | 159824017 0.0046 | 247772383 0.0098 | 180962622 0.0056 | 169535526 0.0050 |
| Methyl Naphthalene (8) Response Volume Absorbed (uL) $y = 1.66E-19x^2 + 1.38E-11x + 1.15E-04$ | 169599557 0.0072 | 176851947 0.0077 | 145781013 0.0056 | 213243790 0.0106 | 135931397 0.0051 | 164792739 0.0069 |
| Tetradecane (9) Response Volume Absorbed (uL) $y = 1.06E-19x^2 + 8.47E-12x + 2.48E-04$ | 126459663 0.0030 | 137199453 0.0034 | 106875883 0.0024 | 177923589 0.0051 | 156452541 0.0042 | 157977240 0.0042 |
| Fuel Volume (uL) Poly Volume (uL) Fuel %, v/v | 0.0337 0.3444 8.91% | 0.0376 0.3794 9.03% | 0.0266 0.2907 8.39% | 0.0556 0.5296 9.50% | 0.0370 0.4318 7.90% | 0.0276 0.2460 10.10% |
| Average Fuel %, v/v | 8.97% | | | | | |



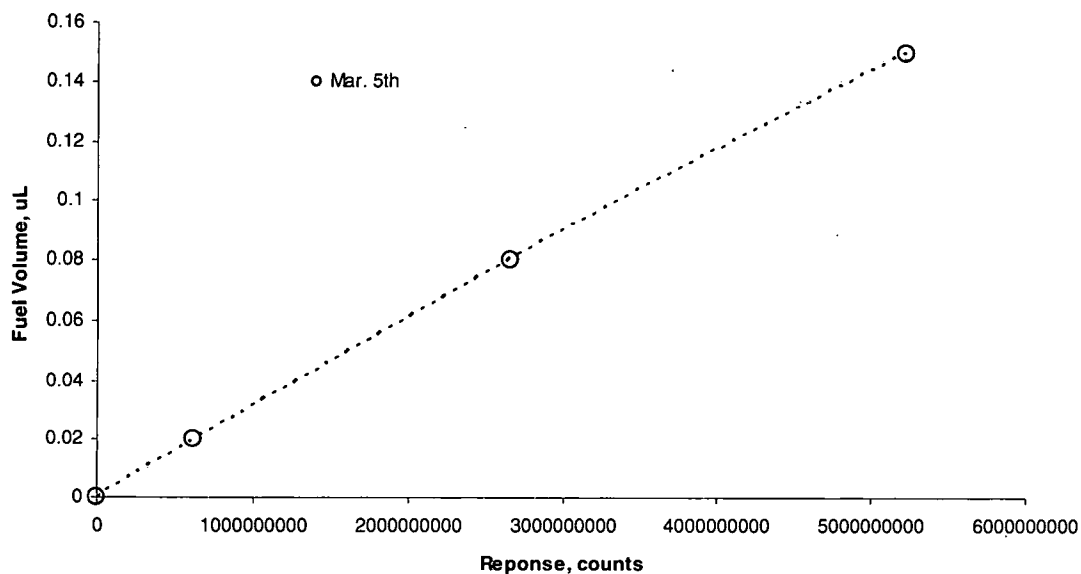
| | FEB2905 | FEB2906 | FEB2907 | FEB2908 |
|---------------------------------------|------------|------------|------------|------------|
| Mass (ug) | 719 | 1768 | 1229 | 977 |
| Response | 2236557647 | 5723687057 | 3922565833 | 2888078482 |
| Fuel Volume Absorbed (uL) | 0.0482 | 0.1263 | 0.0857 | 0.0626 |
| $y = 1.0E-22x^2 + 2.2E-11x - 6.1E-04$ | | | | |
| Poly Volume (uL) | 0.47 | 1.15 | 0.80 | 0.63 |
| Fuel %, v/v | 9.37% | 9.92% | 9.70% | 8.99% |
| Average Fuel %, v/v | 9.49% | | | |

Figure A.13. Calibration curve (above) and calculations (below) for O-ring 1 in FT fuel.



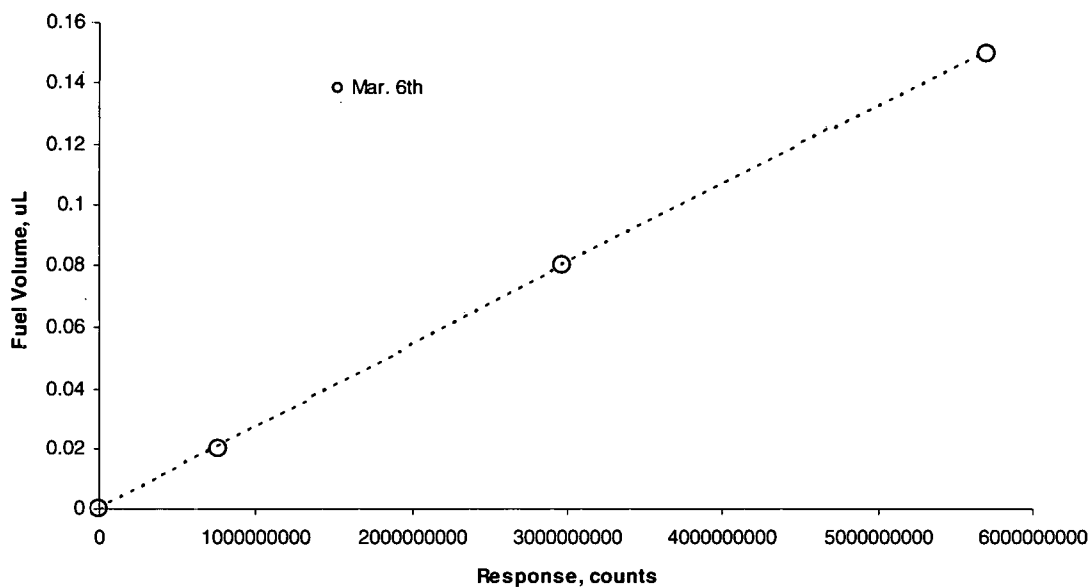
| | MAR0305 | MAR0306 | MAR0307 | MAR0308 | MAR0309 | MAR0310 |
|---|-----------|------------|------------|------------|------------|-----------|
| Mass (ug) | 726 | 1054 | 1446 | 1566 | 975 | 937 |
| Response | 746414883 | 1156659305 | 1664948247 | 1785440188 | 1080764747 | 968263729 |
| Fuel Volume Absorbed (uL) | 0.0399 | 0.0612 | 0.0871 | 0.0931 | 0.0573 | 0.0515 |
| $y = -1.18E-21x^2 + 5.42E-11x + 1.10E-04$ | | | | | | |
| Poly Volume (uL) | 0.47 | 0.68 | 0.94 | 1.02 | 0.63 | 0.61 |
| Fuel %, v/v | 7.81% | 8.22% | 8.49% | 8.39% | 8.31% | 7.81% |
| Average Fuel %, v/v | 8.17% | | | | | |

Figure A.14. Calibration curve (above) and calculations (below) for O-ring 2 in FT fuel.



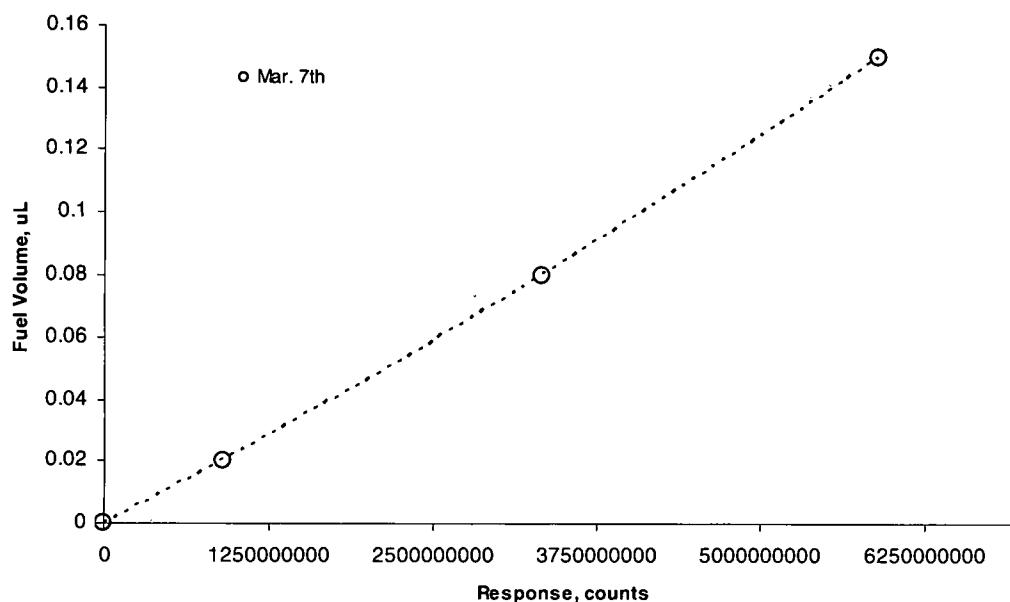
| | MAR0505 | MAR0506 | MAR0507 | MAR0508 | MAR0509 |
|--|------------|------------|------------|------------|------------|
| Mass (ug) | 1335 | 1067 | 1091 | 1181 | 675 |
| Response | 1946817479 | 1648798871 | 1666191473 | 1786604157 | 1069751187 |
| Fuel Volume Absorbed (uL) | 0.0596 | 0.0508 | 0.0513 | 0.0548 | 0.0334 |
| $y = -5.4E-22x^2 + 3.2E-11x + 2.5E-04$ | | | | | |
| Poly Volume (uL) | 0.87 | 0.69 | 0.71 | 0.77 | 0.44 |
| Fuel %, v/v | 6.44% | 6.83% | 6.75% | 6.68% | 7.08% |
| Average Fuel %, v/v | 6.76% | | | | |

Figure A.15. Calibration curve (above) and calculations (below) for O-ring 3 in FT fuel.



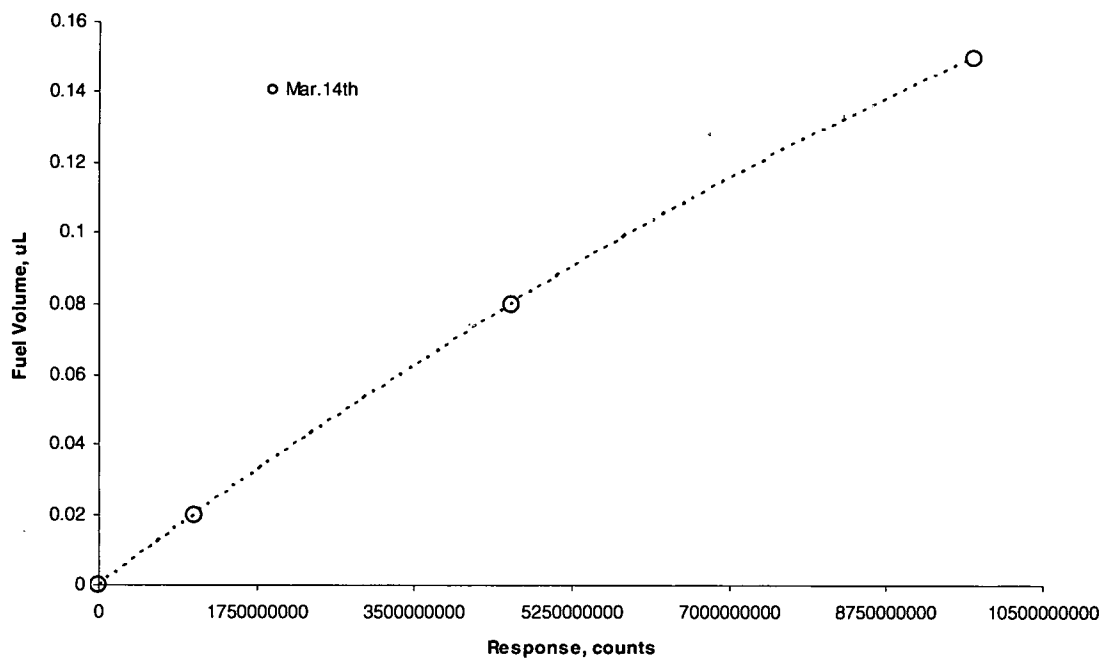
| | MAR0605 | MAR0606 | MAR0607 | MAR0608 | MAR0609 | MAR0610 |
|---|------------|------------|------------|------------|------------|-----------|
| Mass (ug) | 985 | 1269 | 897 | 1483 | 781 | 1265 |
| Response | 1786367267 | 2403044835 | 1777598578 | 2812488620 | 1565102186 | 2.542E+09 |
| Fuel Volume Absorbed (uL) $y = -2.2E-22x^2 + 2.8E-11x - 3.3E-04$ | 0.0484 | 0.0649 | 0.0481 | 0.0757 | 0.0424 | 0.0686 |
| Poly Volume (uL) | 0.64 | 0.82 | 0.58 | 0.96 | 0.51 | 0.82 |
| Fuel %, v/v | 7.04% | 7.30% | 7.64% | 7.30% | 7.73% | 7.71% |
| Average Fuel %, v/v | 7.45% | | | | | |

Figure A.16. Calibration curve (above) and calculations (below) for O-ring 4 in FT fuel.



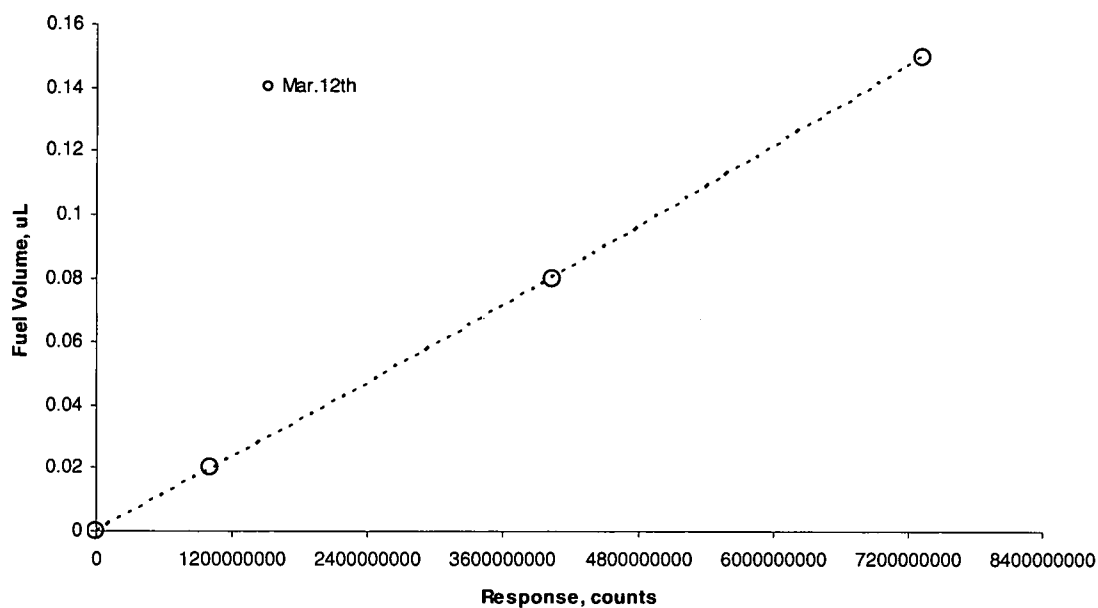
| | MAR0705 | MAR0706 | MAR0707 | MAR0708 | MAR0709 |
|--|------------|------------|------------|------------|------------|
| Mass (ug) | 789 | 900 | 1014 | 1205 | 1362 |
| Response | 2121146703 | 2366353140 | 2583705164 | 3302130984 | 3575792646 |
| Fuel Volume Absorbed (uL) | 0.0496 | 0.0557 | 0.0611 | 0.0794 | 0.0865 |
| $y = 5.47E-22x^2 + 2.23E-11x - 1.68E-04$ | | | | | |
| Poly Volume (uL) | 0.51 | 0.58 | 0.66 | 0.78 | 0.88 |
| Fuel %, v/v | 8.83% | 8.70% | 8.50% | 9.22% | 8.92% |
| Average Fuel %, v/v | 8.84% | | | | |

Figure A.17. Calibration curve (above) and calculations (below) for O-ring 1 in JP-8 fuel.



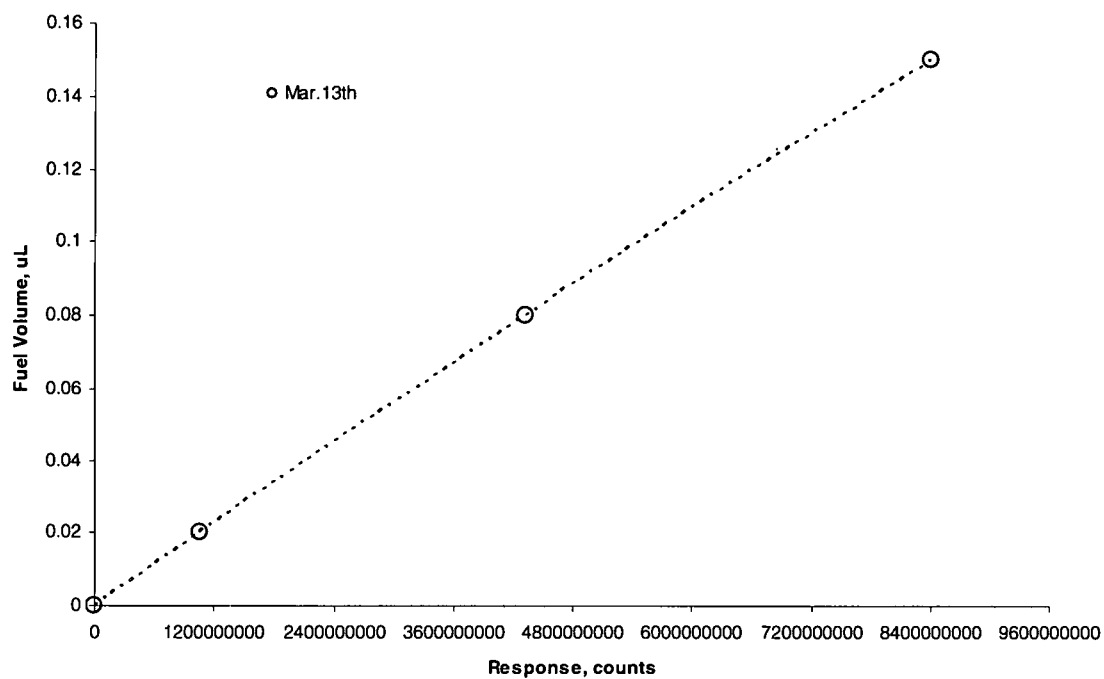
| | MAR1405 | MAR1406 | MAR1407 |
|--|-----------|------------|-----------|
| Mass (ug) | 929 | 1392 | 920 |
| Response | 3.573E+09 | 5560815198 | 3.519E+09 |
| Fuel Volume Absorbed (uL) $y = -4.01E-22x^2 + 1.93E-11x + 2.84E-05$ | 0.0640 | 0.0952 | 0.0631 |
| Poly Volume (uL) | 0.60 | 0.90 | 0.60 |
| Fuel %, v/v | 9.60% | 9.53% | 9.56% |
| Average Fuel %, v/v | 9.57% | | |

Figure A.18. Calibration curve (above) and calculations (below) for O-ring 2 in JP-8 fuel.



| | MAR1205 | MAR1206 | MAR1207 | MAR1208 | MAR1209 |
|--|----------|-----------|-----------|-----------|-----------|
| Mass (ug) | 1297 | 977 | 821 | 730 | 820 |
| Response | 4.29E+09 | 3.242E+09 | 2.745E+09 | 2.396E+09 | 2.778E+09 |
| Fuel Volume Absorbed (uL) | 0.0855 | 0.0640 | 0.0540 | 0.0470 | 0.0546 |
| $y = 2.01E-22x^2 + 1.90E-11x + 2.79E-04$ | | | | | |
| Poly Volume (uL) | 0.84 | 0.63 | 0.53 | 0.47 | 0.53 |
| Fuel %, v/v | 9.22% | 9.17% | 9.20% | 9.02% | 9.31% |
| Average Fuel %, v/v | 9.19% | | | | |

Figure A.19. Calibration curve (above) and calculations (below) for O-ring 3 in JP-8 fuel.



| | MAR1305 | MAR1306 | MAR1307 | MAR1308 | MAR1309 |
|---|-----------|-----------|-----------|-----------|-----------|
| Mass (ug) | 1346 | 761 | 1032 | 800 | 890 |
| Response | 5.101E+09 | 2.788E+09 | 3.835E+09 | 3.002E+09 | 3.431E+09 |
| Fuel Volume Absorbed (uL) | 0.0938 | 0.0522 | 0.0713 | 0.0562 | 0.0640 |
| $y = -1.59E-22x^2 + 1.92E-11x - 1.13E-04$ | | | | | |
| Poly Volume (uL) | 0.87 | 0.49 | 0.67 | 0.52 | 0.58 |
| Fuel %, v/v | 9.70% | 9.57% | 9.62% | 9.76% | 9.97% |
| Average Fuel %, v/v | 9.73% | | | | |

Figure A.20. Calibration curve (above) and calculations (below) for O-ring 4 in JP-8 fuel.

REFERENCES

1. U.S. Department of Energy, Energy Information Administration. *Intl Petroleum Monthly*, January 2008.
2. U.S. Department of Energy, Energy Information Administration. *Intl Energy Outlook – 2005*, July 2005.
3. U.S. Department of Energy, Energy Information Administration.
4. Hubbert, M. King. "Nuclear Energy and the Fossil Fuels," *American Petroleum Institute Drilling and Production Practice Proceedings* (Spring 1956), pp. 5-75.
5. Hubbert, M. King, "Energy Resources," in National Research Council, Committee on Resources and Man, *Resources and Man* (San Francisco: W.H. Freeman, 1969), pp. 196.
6. Deffeyes, Kenneth S. *Beyond Oil: The View From Hubbert's Peak*. New York: Hill and Wang, 2005.
7. Youngquist, Walter. "The Post-Petroleum Paradigm – and Population." *Population and Environment: A Journal of Interdisciplinary Studies*. Volume 20, Number 4, March 1999.
8. *BP, Statistical Review of World Energy*, June, 2006.
9. U.S. Department of Energy, Energy Information Administration. *Monthly Energy Review*, January 2008.
10. The National Economic Council. *Advanced Energy Initiative*, February 2006.
11. Maurice, L. Q. *Fuel*, 2001, 80, pp. 747-759.
12. U.S. Department of Energy, Energy Information Administration. *Annual Energy Review*, 2006.

13. Shanker, Thom. "Military Plans Test in Search for an Alternative to Oil-Based Fuel." *New York Times*, 14 March 2006.
14. Graham, John L., *Energy & Fuels*, 2006, 20, pp. 759-765.
15. Davis, Burtron H., "Fischer-Tropsch Synthesis: Current Mechanisms and Futuristic Needs." *Fuel Processing Technology*, 71 (2001) pp. 157-166.
16. Graham, John L., "A Statistical Approach to Estimating the Compatibility of Alternative Fuels with Materials used in Seals and Sealants." *American Institute of Aeronautics and Astronautics* 2007-5740. 43rd AIAA/ASME/SAE/ASEE Joint Propulsion Conference and Exhibit, Cincinnati, OH. July 8-11, 2007.
17. Miller-Chou, B.A., Koenig, J.L., "A Review of Polymer Dissolution," *Prog. Polym. Sci.*, 28, pp. 1223-1270, 2003.
18. Schwarzenbach, R.P., P.M. Gschwend, and D.M. Imboden., *Environmental Organic Geochemistry*. John Wiley & Sons, 1993.
19. Graham, John L., "A Laboratory Assessment of the Compatibility of Fischer-Tropsch Derived and Blended FT-Petroleum-Derived Fuels with Non-metallic Materials." 10th International Conference on Stability, Handling and Use of Liquid Fuels, October 7-11, 2007.
20. *Standard Test Method for Rubber Property-Effect of Liquids*; Document No. ASTM D 741-98e1; SSTM International: West Conshohocken, PA. 1999.
21. Graham, John L., "Investigation of the Utilization of Undiluted Fischer-Tropsch-Derived Jet Fuels and Mixtures of Fischer-Tropsch-Derived and Petroleum Derived Jet Fuels in Aviation Systems," final report, DOE/NETL Contract Number DE-A126-01NT4110, December, 2006.
22. Chevron Phillips Chemical Company LP. Hydrocarbon Fluid Type I. Material Safety Data Sheet 26090.
23. Chevron Phillips Chemical Company LP. Hydrocarbon Fluid Type III. Material Safety Data Sheet 40490.
24. Bacha, J., Barnes, F., Franklin, M., Gibbs, L., Hemighaus, G., Hogue, N., Lesnini, D., Lind, J., Maybury, J., and Morris, J., *Aviation Fuels Technical Review*, Chevron Products Company, Houston, TX, 2000.
25. Striebach, R.C., Rubey, W.A., "A System for Thermal Diagnostic Studies." American Laboratory. January, 1990.

R002593887